

Abundance variations in the globular cluster M71 (NGC 6838)

A. Alves-Brito¹, R. P. Schiavon², B. Castilho³, and B. Barbuy¹

¹ Universidade de São Paulo, IAG, Rua do Matão 1226, Cidade Universitária, São Paulo 05508-900, Brazil
e-mail: abrito@astro.iag.usp.br, barbuy@astro.iag.usp.br

² Department of Astronomy, University of Virginia, P.O. Box 3818, Charlottesville, VA 22903-0818.
e-mail: rps7v@mail.astro.virginia.edu

³ Laboratório Nacional de Astrofísica/MCT, CP 21, Itajubá, MG, 37500-000, Brazil
e-mail: bruno@lna.br

2007

ABSTRACT

Context. Abundance variations in moderately metal-rich globular clusters can give clues about the formation and chemical enrichment of globular clusters.

Aims. CN, CH, Na, Mg and Al indices in spectra of 89 stars of the template metal-rich globular cluster M71 are measured and implications on internal mixing are discussed.

Methods. Stars from the turn-off up to the Red Giant Branch ($0.87 < \log g < 4.65$) observed with the GMOS multi-object spectrograph at the Gemini-North telescope are analyzed. Radial velocities, colours, effective temperatures, gravities and spectral indices are determined for the sample.

Results. Previous findings related to the CN bimodality and CN-CH anticorrelation in stars of M71 are confirmed. We also find a CN-Na correlation, and Al-Na, as well as an Mg₂-Al anticorrelation.

Conclusions. A combination of convective mixing and a primordial pollution by AGB or massive stars in the early stages of globular cluster formation is required to explain the observations.

Key words. globular clusters : general – globular cluster : individual : M71 – stars : abundances

1. Introduction

Globular Clusters (GCs) provide important information on the early chemical and dynamical evolution of the Milky Way.

Star-to-star abundance variations of light elements - Li, C, N, O, Na, Mg, and Al - are extensively reported in the literature (Gratton et al. 2004 and references therein). Li variations among turnoff (TO) stars and a Li-Na anticorrelation have been reported; among giant stars, C and N abundances, as well as the pairs O:Na and Al:Mg are also found to be anticorrelated. Such anomalies have not been obtained for heavier elements. These abundance variations have been reported in the literature over the past two decades, but their origin is still widely debated.

Some of the abundance variations seen in globular-cluster giants can be explained by evolutionary mixing with migration of processed material through the CNO cycle to the surface of giant stars (Iben 1964; Charbonnel 1994), whereas a primordial-enrichment scenario, which requires early contamination of intra-cluster material, is claimed by some authors (e.g. Smith 1987; Kraft 1994).

With a moderately high metallicity ($\langle [Fe/H] \rangle = -0.73$, Harris 1996), and an old age of 10-12 Gyr (Grundahl et al. 2002; Meissner & Weiss 2006), M71 is often regarded as a prototype of northern metal-rich globular clusters and considered as a suitable globular cluster to study abundance variations. It is located near the Galactic plane ($b = -4.6^\circ$) and has a reddening of $E(B-V) = 0.27 \pm 0.05$ and an apparent distance modulus of $(m-M)_V = 13.60 \pm 0.10$ (Geffert & Maintz 2000). Dinescu et al. (1999) have obtained space velocities for a set of Galactic globular clus-

ters. For M71 they determined velocity components (U, V, W) = $(77 \pm 14, -58 \pm 10, -2 \pm 14)$ km/s and a low eccentricity orbit, which characterizes M71, kinematically, as a thick-disk cluster.

Chemical abundances were discussed in several previous studies of this cluster, including DDO photometry of giant stars (Hesser et al. 1977; Briley et al. 2001) and low- and high-resolution analysis of stars in different evolutionary stages from the Main-Sequence (MS) TO to the Red Giant Branch (RGB) tip (Cohen 1980; Smith & Norris 1982; Leep et al. 1987; Smith & Penny 1989; Penny et al. 1992; Sneden et al. 1994; Cohen 1999; Ramirez & Cohen 2002; Lee et al. 2004; Lee 2005; Boesgaard et al. 2005; Yong et al. 2006). Many of these studies show a CN bimodality, with CN-CH anticorrelation, Na-O anticorrelation and variations in Al abundance.

In this paper we present the main results of an analysis of high S/N, medium resolution, Gemini/GMOS spectra of a large number of M 71 stars, from the main-sequence turnoff to the tip of the giant branch. Our goals are twofold: to improve the statistics on abundance variations in M71 stars; and to study the behaviour of 14 spectral indices for the sample stars in order to shed light on the main astrophysical processes leading to the observed star-to-star abundance variations. We estimate the C and N abundances of one CN-strong and one CN-weak giant from spectrum synthesis, based on state-of-the-art model photospheres and an up-to-date line list. A comparison of our results with those based on recent high-resolution abundance analysis is also presented.

This paper is structured as follows. The observations and data reductions are described in Sect. 2. The analysis of radial velocities, photometry, atmospheric parameters and line indices

is presented in Sect. 3. In Sect. 4 the results are shown, and in Sec. 5 they are discussed and contrasted with previous studies. Our conclusions are summarized in Sect. 6.

2. Observations and data reduction

Imaging and spectroscopy of M71 stars were obtained with the Gemini Multi-Object Spectrograph (GMOS; see, for example, Hook et al. 2004 for more details) in the MOS mode on the 8m Frederick C. Gillett Telescope (Gemini-North).

On July 18, 2002, the pre-imaging required to build four GMOS masks was obtained. It superposes a GMOS-North field over 5.5 arcmin x 5.5 arcmin. The image of the M71 field was obtained using the r_G0303 filter, with an effective wavelength of 6300 Å and wavelength coverage of 5620-6980 Å. Exposures of 4 x 180s were taken, with the CCD detector operating at 4 electrons/DN and a readout noise of 6.6 electrons. The mean airmass during the pre-imaging observation was 1.157. Thus, using a finding-chart available in Cudworth (1985), 145 M71 stars were identified in the GMOS image and selected for spectroscopic observations.

Spectroscopic data were collected on August 5, 2002, using the B600+_G5303 (600 lines/mm) grating and adopting arcsec-wide slits. The CCDs were binned in a 2 x 2 mode (along both the spatial and dispersion axes). This configuration achieved a spectral resolution $R \sim 2,000$ at 5100 Å with a dispersion of 0.0917 nm/pix, covering from 3500 to 7000 Å.

The 145 target stars were selected in order to give appropriate sampling of the colour magnitude diagram (CMD). The maximum time for each individual exposure was constrained by the bright red giants of the cluster. Short exposures were taken in order to avoid saturation and a number of these exposures for the faintest stars of the turn-off were co-added. The total integration time was defined by our desire to achieve $S/N \sim 150$ at $\lambda \sim 4000$ Å. Finally, spectra of the spectrophotometric standard star EG 131 were obtained using a 1-arcsec longslit, with the same instrumental set up as adopted for the science observations.

Science and standard star data were both reduced using the GEMINI GMOS Data Reduction Package within the IRAF package. Bias frames, flat-fields and CuAr images were taken as part of the GEMINI base calibrations. At this point, the reduction process comprised bias-subtraction and flat-fielding, using GCAL flats which were previously co-added and normalized. Cosmic rays were then cleaned. The wavelength calibration was carried out with solutions obtained from the CuAr arc exposures, which provided typical residuals of 0.2 Å. Spectra were then sky-subtracted and extracted into a series of 1D spectra. All spectra were extinction-corrected using the mean extinction coefficients obtained for Mauna Kea. As a result of the location of the *slits* with respect to the mask-bisector, the wavelength coverage varies from star to star. In addition, two gaps corresponding to 0.5mm between CCDs are also present in the final spectra.

3. Analysis

3.1. Heliocentric radial velocities

Heliocentric radial velocities for the sample stars were obtained using both *rvidlines* and *fxcor* IRAF procedures. The former measures radial velocities from spectra by determining the wavelength shift in spectral lines relative to specified rest wavelengths and the measured velocities are corrected to a heliocentric frame of reference. We derived a mean heliocentric radial velocity of

-12 ± 46 km/s ($N = 145$ stars). The task *fxcor*, on the other hand, performs a Fourier cross-correlation between lists of input object and template spectra. A set of 77 spectral templates with stellar parameters given by: $[\text{Fe}/\text{H}] = -1.00$, $[\alpha/\text{Fe}] = 0.00$, $4250 \leq T_{\text{eff}} \leq 5750$ K and $0.00 \leq \log g \leq 5.0$ dex were taken from the library of synthetic stellar spectra by Coelho et al. (2005). Measurements of 142 stars led to a mean heliocentric radial velocity of 11 ± 49 km/s.

The mean difference between the heliocentric radial velocities as measured in two ways ($v_{\text{fxcor}}^{\text{h}} - v_{\text{rvidlines}}^{\text{h}}$) is 23 km/s. For comparison, Harris (1996) gives a mean heliocentric radial velocity of -22.8 ± 0.2 km/s for M71. As the sample spectra have a resolution $R \sim 2000$, we expect a theoretical accuracy of around $(1/10)(c/2000) = 15$ km/s, which is in good agreement with the scatter obtained above. Individually, the higher values in the measurements of the heliocentric radial velocities could be explained in part based on the low-resolution of the spectra. We found a nearly Gaussian distribution of the radial velocities with a dispersion of ~ 45 km/s, and we believe that this finding reflects the uncertainty in the determination of the radial velocity itself at this spectral resolution. The accuracy in the heliocentric radial velocities measurements is also wavelength-calibration dependent; in our case the GMOS calibration lamps were rather poor. Given the high velocity-dispersion obtained, the radial velocities were used to shift the sample spectra to rest wavelengths rather than a star membership selection criterion.

3.2. Photometry

As reported in the GEMINI/GMOS web site¹, up to September 12, 2006 there was a large ($\sim 5''$) offset in the optical positions (RA and DEC) in GMOS-North images. A FORTRAN code was applied in order to take these offsets into account and find out the correct identification of the sample stars from previous photometric catalogs of M71. Using the *SkyCat* tool we plotted all 145 observed stars on the Gemini-North preimaging and created our own finding chart of M71 following the identification as given in each GMOS mask. Optical photometry for M71 from the literature was adopted by selecting CCD photometry able to give us crucial information like completeness and membership probability. Two papers fulfilled these requirements: (i) Cudworth (1985) presents proper motions and visual photometry for 350 M 71 stars down to a limit of $V = 16$. Cudworth (2006, priv. comm.) gives proper motions and photometry for fainter stars ($V > 16$), amounting to 1522 stars. (ii) Geffert & Maintz (2000) and Geffert (2002, priv. comm.) present B,V CCD observations for around 4450 stars (limited to $V = 18.5$ mag) covering a field of 20 x 20 arcminutes of M71.

The colour-magnitude diagram (CMD) of M71, using the photometry from Cudworth (1985, 2006) and marking the sample stars is displayed in Figure 1. Overplotted is a Yonsei-Yale isochrone (Kim et al. 2002) with parameters $[\text{Fe}/\text{H}] = -0.68$ dex, $[\alpha/\text{Fe}] = 0.00$ dex, age = 12 Gyr. The isochrone has been shifted by $(m-M)_V = 13.60$ mag and $E(B-V) = 0.27$ mag (Geffert & Maintz 2000). The stars' designations, positions, membership probabilities, colours, along with bolometric magnitudes, gravities and temperatures are shown in Table 1.

3.2.1. Temperatures

Effective temperatures (T_{eff}) for the sample were obtained by employing the empirical calibrations of Alonso et al. (1996;

¹ <http://www.gemini.edu/sciops/instruments/gmos/gmosIndex.html>

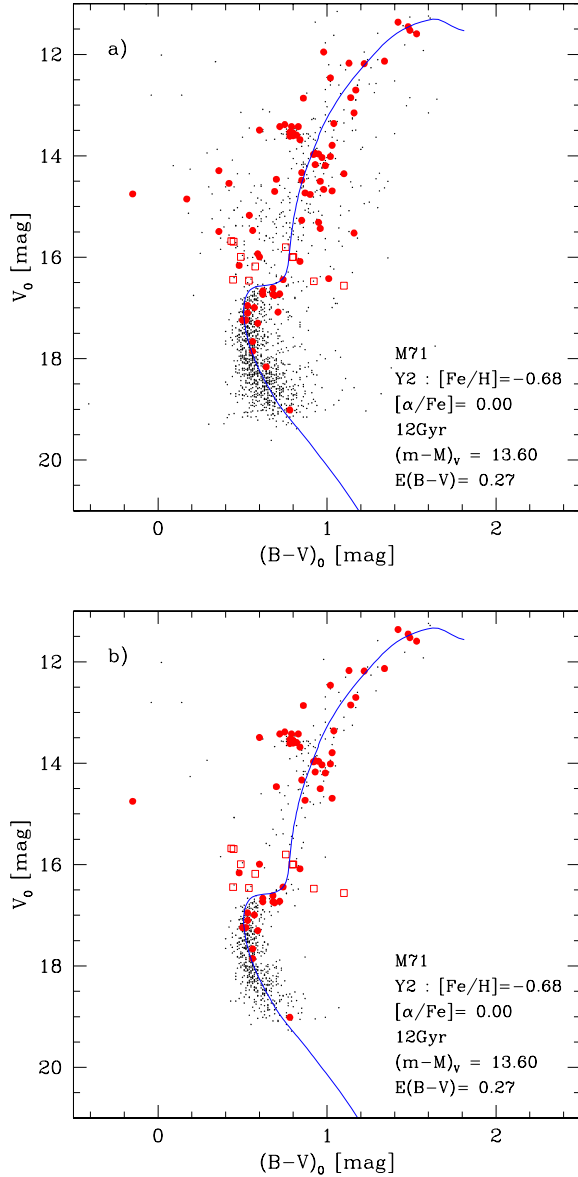


Fig. 1. The optical V,B-V CMD of M71. *Top*: dots: Cudworth (1985,2006) photometry; filled circles: sample stars; open squares: stars identified in Geffert & Maintz (2000). *Bottom*: stars with membership probability $P \geq 80\%$ (symbols are the same as above). A Yonsei-Yale isochrone by Kim et al. (2002) with parameters as indicated is overlotted.

1999; 2001) for dwarfs and giants stars. The intrinsic colours $(B-V)_0$ were determined by adopting $E(B-V) = 0.27$ (Geffert & Maintz 2000) and mean $[Fe/H] = -0.73$ (Harris 1996). The uncertainty in the effective temperatures $T(B-V)$ derived using Alonso et al.’s calibrations is typically 150 K (within 1σ).

3.2.2. Surface gravities

Photometric gravities for all stars were obtained in the classical way, using the T_{eff} s described in the previous section and adopting $M_* = 0.80 M_{\odot}$, $(m-M)_V = 13.60$, $E(B-V) = 0.27$ (Geffert & Maintz 2000), with bolometric corrections taken from Alonso et al. (1999). Input solar values adopted were: $T_{\odot} = 5780$ K, $M_{\text{bol}\odot} = 4.75$, and $\log g = 4.44$. The error in M_{bol} is mostly due

to the M_V value and total extinction A_V , the latter with an uncertainty around ± 0.05 mag. For M_V , adopting an error in distance as large as 30%, we get $\sigma_{M_{\text{bol}}} \sim 0.30$ mag, which leads to an error on the adopted photometric gravities of ± 0.30 dex. For stars fainter than $V = 17.5$, the surface gravities were derived from Yonsei-Yale 12 Gyr isochrones of $Z=0.0040$, $Y = 0.24$ and $[Fe/H] = -0.70$ (Kim et al. 2002).

3.2.3. Spectral indices

The ability to analyze individual spectra of cluster members can provide knowledge on the spectral properties of stellar populations, placing constraints on stellar population synthesis. In medium-resolution spectra the measurement and analysis of spectral indices is widely employed to interpret the chemical evolution history of stellar populations in galaxies.

Absorption line indices were measured using the LECTOR program, by A. Vazdekis, which measures line strengths in 1-D spectra (Vazdekis et al. 2003). Besides measuring the Lick/IDS absorption-line indices (Worthey et al. 1994; Worthey & Ottaviani 1997) we modified LECTOR in order to measure the line indices recently defined by Serven et al. (2005). In this paper, the only index from the latter list we will discuss is A13953, which was shown by Serven et al. to be very sensitive to the abundance of aluminium.

For the uncertainties on the indices we initially considered those provided by LECTOR (see Cardiel et al. 1998 for details). These Poisson-based uncertainties on the indices are underestimated. Thus, the uncertainties were also estimated from the standard deviation of the measurements for each index on the individual spectra, and hereafter these latest uncertainties will preferentially be shown.

In Table 2 are presented the index passband definitions where wavelengths are given in angstroms. Tables 3, 4 and 5 show the results and Poisson uncertainties in the total-passband net counts for the indices CN_1 [mag], CN_2 [mag], $Ca4227$ [Å], $G4300:CH$ [mag], $Fe4383$ [Å], H_{β} [Å], Mg_1 [mag], Mg_2 [mag], Mgb [Å], $Fe5270$ [Å], $Fe5335$ [Å], $Fe 5406$ [Å], NaD [Å] and A13953 [Å], while Figure 2 shows one of the final flux-calibrated spectra of the sample with some features labeled.

4. Results

The final sample adopted consists of stars with a membership probability higher than 80% and magnitudes $V \leq 15.5$ mag. In addition, each spectrum was individually inspected by the region of the index passbands. Below we present the main results.

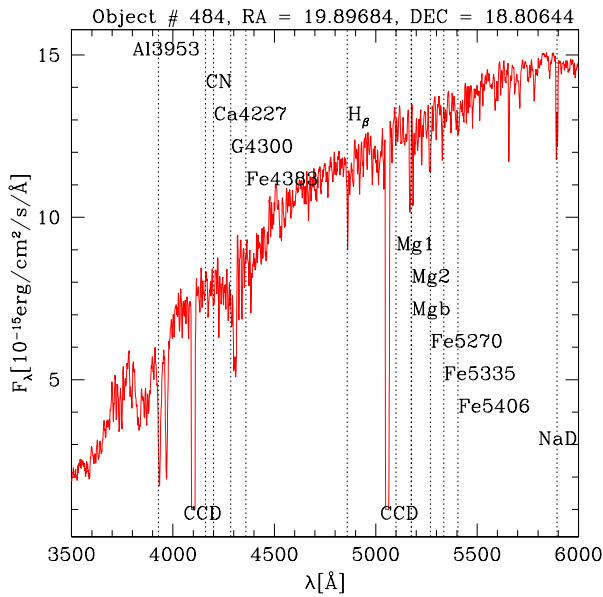
4.1. CN and CH

The Lick CN indices measure the strength of the CN 4150 Å bandhead. Although we have measured CN_1 and CN_2 , we chose to work with CN_1 more extensively. Both indices are similar in definition with a slight difference in their blue pseudocontinuum definition.

Figures 3a,b present the CN_1 index vs. V-band magnitude and $(B-V)_0$ colours for M71 selected stars. Stellar IDs are also marked. The distribution of the data points in these two plots is clearly bi-modal, with two families of stars with strong and weak CN bands at fixed colour and/or magnitude. The dividing line between CN-strong stars, in the top half, and CN-weak stars in the bottom half of the plots runs diagonally from the lower left to the top right of both plots. This is because in both families of

Table 2. Index definition.

Index	Blue Pseudocontinuum	Feature	Red Pseudocontinuum
(1)	(2)	(3)	(4)
CN ₁	4081.375 4118.875	4143.375 4178.375	4245.375 4285.375
CN ₂	4085.125 4097.625	4143.375 4178.375	4245.375 4285.375
Ca4227	4212.250 4221.000	4223.500 4236.000	4242.250 4252.250
G4300	4267.625 4283.875	4282.625 4317.625	4320.125 4336.375
Fe4383	4360.375 4371.625	4370.375 4421.625	4444.125 4456.625
H_beta	4827.875 4847.875	4847.875 4876.625	4876.625 4891.625
Mg ₁	4895.125 4957.625	5069.125 5134.125	5301.125 5366.125
Mg ₂	4895.125 4957.625	5154.125 5196.625	5301.125 5366.125
Mgb	5142.625 5161.375	5160.125 5192.625	5191.375 5206.375
Fe5270	5233.150 5248.150	5245.650 5285.650	5285.650 5318.150
Fe5335	5304.625 5315.875	5312.125 5352.125	5353.375 5363.375
Fe5406	5376.250 5387.500	5387.500 5415.000	5415.000 5425.000
NaD	5862.375 5877.375	5878.625 5911.125	5923.875 5949.875
Al3953	3937.600 3967.400	3921.300 3935.500	3969.500 3987.000

**Fig. 2.** Spectrum of the star 484 (1-55, $V = 14.26$) observed in the Mask # 2. Gaps are due to the 3 CCD configuration of the detector. Central wavelengths of studied indices are indicated.

stars, CN is a strong function of temperature, so that CN-bands become stronger for lower temperatures in both the CN-strong and CN-weak groups. It is interesting that stars 291, 390 and 526 are AGB members, and they show a higher N enhancement.

Concerning stars 1351, 1556 and 640, their CN measurements were slightly affected by the presence of the 2 CCD gaps around their red passband. For the CN-strong stars, showing nitrogen excesses, we found $\langle \text{CN} \rangle = 0.19 \pm 0.04$ ($N = 8$ stars), whereas for the CN-weak stars $\langle \text{CN} \rangle = 0.04 \pm 0.04$ ($N = 20$ stars). Note that stars 1351, 1556 and 640 were not taken into consideration in computing the mean CN-weak value.

In Fig. 4 we show the location of CN-strong and CN-weak stars in the CMD, for $V < 15.5$. Stars weaker than $V > 15.5$ are also plotted, with no distinction between CN intensities, given the lower S/N of the spectra. In Fig. 5 the CN₁ index vs. T_{eff} is shown for the giants, where the bimodality of CN-strength is found among both RGB and Asymptotic Giant Branch (AGB) stars. Fig. 6 shows CN₁ vs. $\log g$ for all stars, illustrating the clear separation between CN-strong and CN-weak giants, whereas for

dwarfs, the bimodality is not so clear, partly due to the lower S/N of our dwarf-star spectra, and partly because the differences between CN-strong and CN-weak spectra are more subtle, given that CN-bands are weak overall in the spectra of warm turnoff stars. Recall however that Cohen (1999) has found a bimodality for main sequence (MS) stars of M71.

The G-band at 4300 Å includes a CH bandhead and can be used to derive the carbon abundance. Its behaviour along the main sequence, subgiant and red giant sequences can give important clues on mixing processes along stellar evolution. In Fig. 7 we plot the G band indices as a function of V magnitude. The symbols are the same as used in Figs. 3a,b, where the CN-strong and CN-weak sequences are represented by filled and open circles. One can see that CN-strong stars tend to present lower CH values, while the CN-weak stars appear to show higher values of CH. This general trend confirms the well-known CN-CH anticorrelation in giant stars reported in past decades for many Galactic globular clusters (e.g., Dickens et al. 1979; Smith 1987; Kraft 1994; Gratton et al. 2004 and references therein). Note, however, that despite their high membership probabilities, stars 2001, 458, 505 and 7498 present lower G-band strengths than other CN-weak stars of the sample. Stars 2001, 458 and 505 are HB members, and this suggests that we also detect a bimodal distribution in the HB. Figure 8 plots an example of CN-bimodality and CN-CH anticorrelation for two M71 stars of similar V magnitude and T_{eff} . The CN-strong giant 390 ($T = 4435$ K : $\text{CN} = 0.24$: $\text{CH} = 6.18$) presents a stronger CN band and a weaker CH band strength than star 399 ($T = 4419$ K : $\text{CN} = 0.04$: $\text{CH} = 6.62$).

4.2. Iron and magnesium indices

We measured spectral indices sensitive to the abundances of iron (Fe4383, Fe5270, Fe5335, and Fe5406) and magnesium (Mg₁, Mg₂ and Mgb) in all our spectra. We henceforth focus on an average Fe index, defined as $\langle \text{Fe} \rangle = (\text{Fe4383} + \text{Fe5270} + \text{Fe5335} + \text{Fe5406})/4$ and Mg₂. All these indices are of widespread use in stellar population studies in galaxies and stellar clusters. Figure 9 plots the behaviour of Mg₂ as a function of CN and T_{eff} , respectively. In this figure we see that both CN-weak and CN-strong sequences correspond to $\text{Mg}_2 \geq 0.05$ mag and Mg₂ tends to be higher for cooler stars ($T_{\text{eff}} \leq 4300$ K). Therefore, Mg₂ is weaker in CN-strong stars, and this seems to indicate that besides a Mg-Al anticorrelation (Fig. 14), and a weak Al-CN anticorrelation (Fig. 13), we found some evidence for a Mg-N anticorrelation (see Gratton et al. 2004).

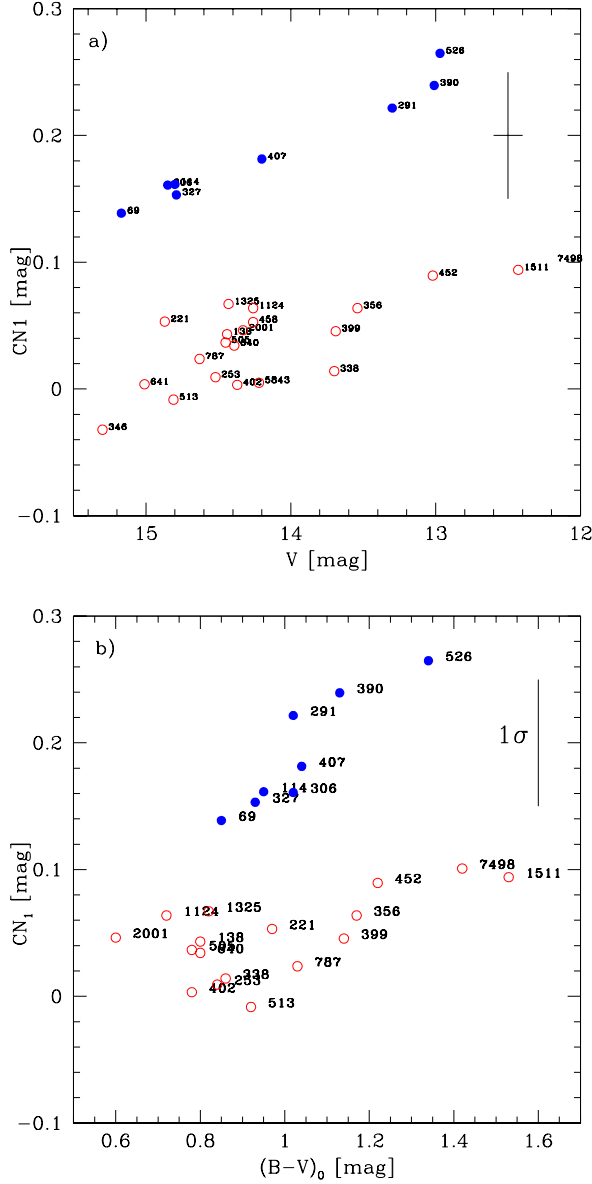


Fig. 3. *a)* CN_1 plotted against V , and *b)* CN_1 vs. $(B-V)_0$ for the M71 sample stars, where the locus CN-strong (*filled circles*) and CN-weak (*open circles*) are seen. Error bars quoted correspond to the rms on all measurements available.

4.3. $Ca4227$

This index is widely used in stellar population studies in galaxies, where Ca is considered as a representative α -element (e.g. Thomas et al. 2003; Prochaska et al. 2005). We found $\langle Ca4227 \rangle = 1.25 \pm 1.00 \text{ \AA}$ for 32 stars in the range $12 \leq V \leq 15.5$ and with a membership probability higher than 80%.

Figures 10 and 11 show the behaviour of $Ca4227$ as a function of T_{eff} and the metallicity indicators $\langle Fe \rangle$ and Mg_2 indices, respectively. By comparing Fig. 9 with Fig. 10, a similarity between the general behaviour of $Ca4227$ and Mg_2 indices with T_{eff} is seen. This explains the behaviour presented between $Ca4227$ and Mg_2 in Fig. 11. All these findings show that the cooler giants with higher metallicity indicators also show high $Ca4227$ indices. These figures also show that the metallicity indices Mg_2 and $\langle Fe \rangle$ grow non-linearly at low temperatures.

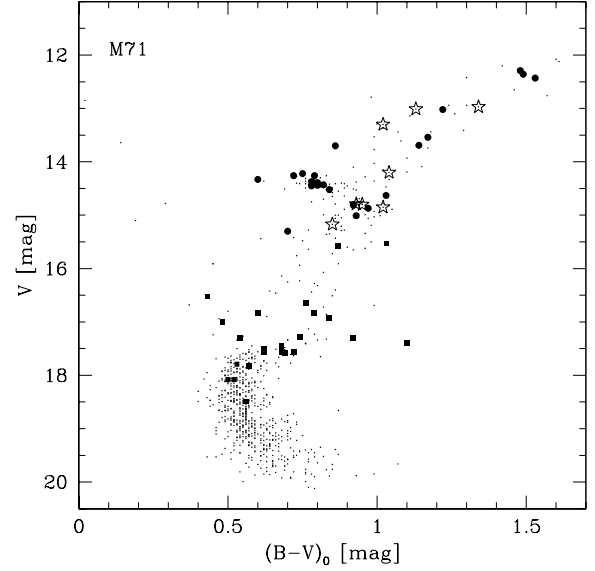


Fig. 4. V , $B-V$ CMD with the CN-strong stars (*open stars*), CN-weak (*filled circles*), and the subgiants (*filled squares*) for which the CN measurements are not qualified as strong or weak.

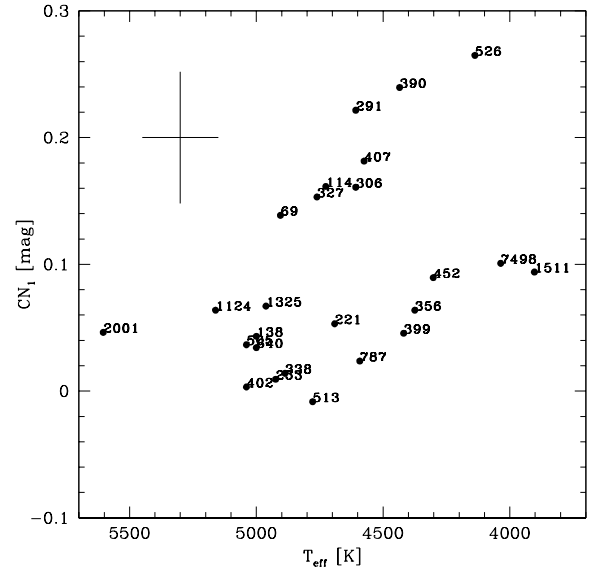


Fig. 5. CN_1 vs. effective temperature. Error bar on CN_1 is as explained in Fig. 3, while on T_{eff} it resembles the value determined with the photometric calibration employed.

4.4. H_β

H_β index is widely used as an age indicator in stellar population studies and is known to be extremely temperature- and gravity-dependent. We found a mean H_β index of $\langle H_\beta \rangle = 1.57 \pm 0.68 \text{ \AA}$ ($N = 31$). We notice that there is a large variation of H_β measurements for stars with $V < 14$ and this effect appears to be real since Figs. 12a,b suggest a higher dispersion on the H_β measurements for stars cooler than 4500 K.

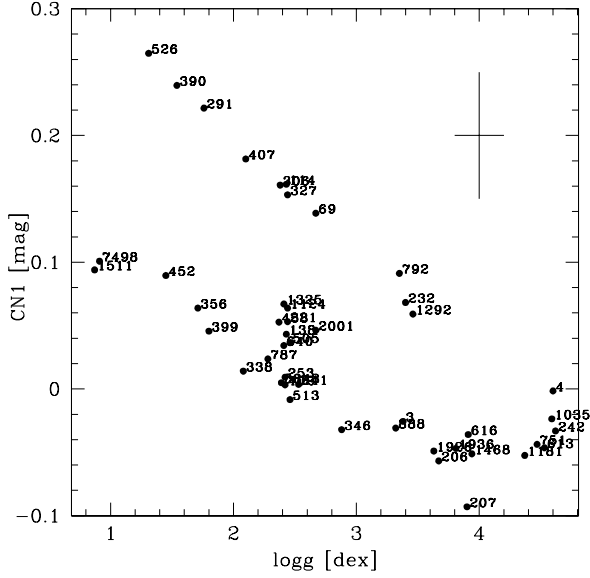


Fig. 6. CN₁ vs. log g. Error bar is indicated.

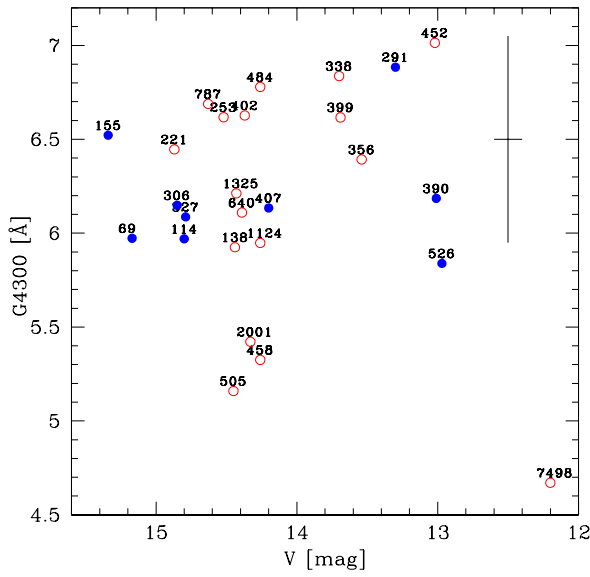


Fig. 7. G-band as function of V magnitude, where CN-strong (filled circles) and CN-weak (open circles) stars are plotted separately.

4.5. NaD and Al3953

NaD and Al3953 features included in the present analysis are as defined in Worthey et al. (1994) and Serven et al. (2005), respectively. As shown in Table 2 of Serven et al. (2005), the new index Al3953 has a high spectral response to aluminum abundance variations. However, although both are very useful indices able to rule out important clues for understanding the abundance variations in stellar populations, they are composed of resonance lines and subject to effects from interstellar absorption, that have to be taken into account when trying to interpret them. We found $\langle \text{NaD} \rangle = 4.60 \pm 2.38 \text{ \AA}$ ($N = 28$) and $\langle \text{Al3953} \rangle = 2.76 \pm 1.35 \text{ \AA}$ ($N = 25$).

Figure 13 displays the behaviour of NaD and Al3953 as a function of the CN band, while Fig. 14 shows the behaviour of

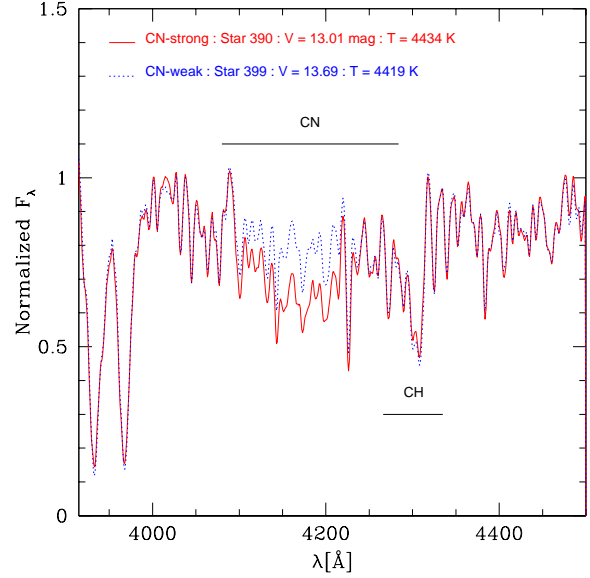


Fig. 8. Stars 390 and 399 in the molecular CN and CH band region. The full and dashed lines represent the CN-strong and CN-weak stars, respectively. These stars display approximately the same temperatures.

NaD and Mg₂ indices against the new index Al3953. An Na-Al anticorrelation is clearly seen.

4.6. Fitting functions

The fitting functions approach is a useful tool at low resolution to derive abundances that are both reddening and distance modulus independent. In this section, we use the fitting functions derived by Barbuy et al. (2003) for the indices Fe5270, Fe5335 and Mg₂, as a function of stellar parameters, in order to estimate metallicities for M 71 stars, based on the Lick index measurements presented in the previous sections.

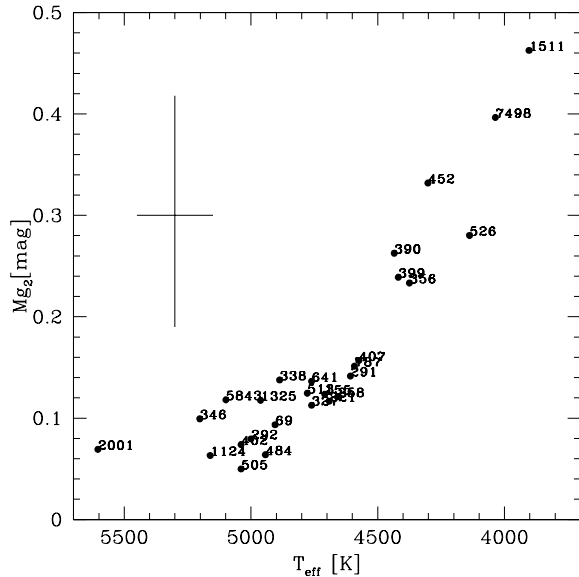
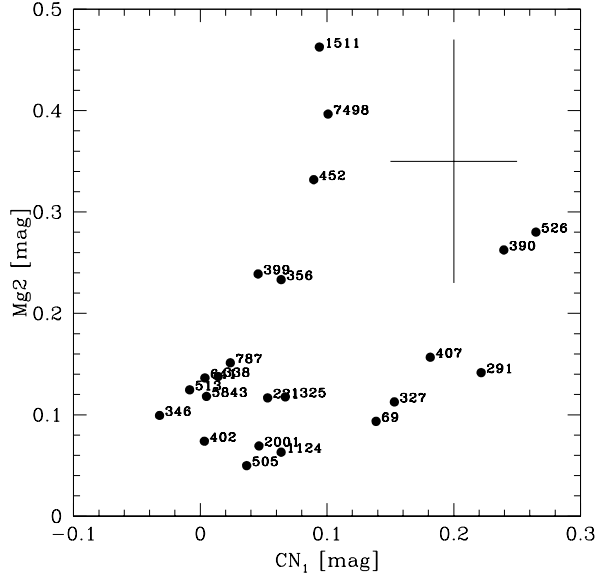
The Fe5270, Fe5335 and Mg₂ features are known to be suitable metallicity indicators due to their relatively weak dependence on gravity and temperature. A relation between these indices and $[\text{Fe}/\text{H}]$ was derived by Barbuy et al. (2003) based on synthetic spectra for resolutions of 8.3 Å and 3.5 Å. We use their Value1 fitting function coefficients for Fe5270, Fe5335 and Mg₂ computed with FWHM = 3.5 Å, valid for $-3 \leq [\text{Fe}/\text{H}] \leq +0.3$, $0 \leq \log g \leq 3$ and $4000 \leq T_{\text{eff}} \leq 7000$.

A mean $\text{Fe} = (\text{Fe5270} + \text{Fe5335})/2$ and Mg₂ indices were used as metallicity indicators. Mean values of $\langle \text{Fe5270} \rangle = 2.70 \pm 1.47$ ($N=30$), $\langle \text{Fe5335} \rangle = 2.53 \pm 1.48$ ($N=29$) and $\langle \text{Mg}_2 \rangle = 0.17227 \pm 0.11828$ ($N = 28$) were obtained for giants. Based on stars in the range $4500 < T_{\text{eff}} < 5000 \text{ K}$ (validity of the fitting functions for Mg₂, mean values of $\text{Fe5270} = 2.21 \pm 0.72$ (18 giants), $\text{Fe5335} = 2.04 \pm 0.63$ (17 giants) and $\text{Mg}_2 = 0.12 \pm 0.03$ (11 giants) are found.

Adopting mean parameters $T_{\text{eff}} = 4768 \text{ K}$ and $\log g = 2.29$ dex, metallicities of $[\text{Fe}/\text{H}] = -0.81$, -0.91 and -0.68 , corresponding to Fe5270, Fe5335 and Mg₂ respectively, are obtained. In Table 6 are reported $[\text{Fe}/\text{H}]$ values from high-resolution spectroscopy and those from fitting functions, where a good agreement is found.

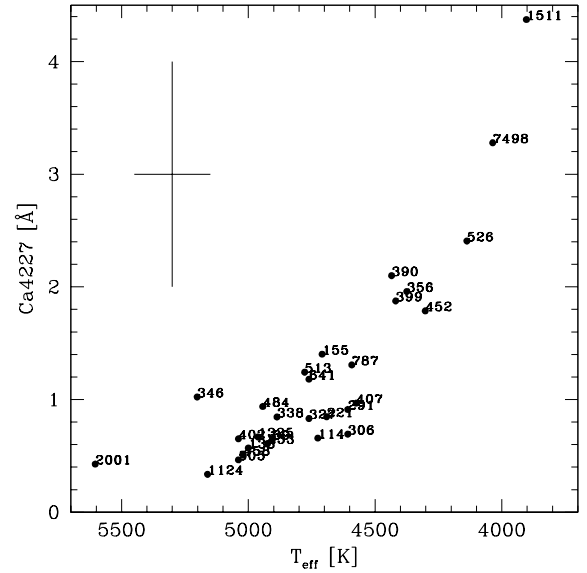
Table 6. Literature and present values of metallicity for M71

[Fe/H]	[FeI/H]	[FeII/H]	Method	Reference
-0.79	-0.79	-0.79	High-resolution : 10 giants	Sneden et al. (1994)
-0.73	—	—	Compilation	Harris (1996)
-0.71	-0.71	-0.84	High-resolution : 25 stars	Ramirez et al. (2001)
-0.82	-0.81	-0.82	Revision of Sneden et al.'s 10 giants	Kraft & Ivans (2003)
-0.80	-0.81	-0.85	High-resolution : 5 dwarfs	Boesgaard et al. (2005)
-0.81	—	—	Fitting Functions	Fe5270 index (Present work)
-0.91	—	—	Idem	Fe5335 index (Present work)
-0.68	—	—	Idem	Mg ₂ index (Present work)

**Fig. 9.** Upper panel: Mg₂ plotted against CN₁; Lower panel: Mg₂ as a function of the effective temperature. Error bars are as previously discussed.

4.7. Spectrum synthesis

By adopting $[\text{Fe}/\text{H}] \approx -0.8$ for M71, taking into account the values given in Table 6, we carried out a spectrum synthesis calculation of CN and CH bands in the wavelength region 4000-4400

**Fig. 10.** Ca4227 feature against the effective temperature.

Å. The code is described by Cayrel et al. (1991) and Barbuy et al. (2003), where CN and CH line lists are from Kurucz (1993), and implemented in our code as described in Castillo et al. (1999). MARCS model atmospheres from Gustafsson et al. (2006) were used.

Synthetic spectra were computed for a pair of CN-weak/CN-strong stars with similar stellar parameters: stars 390 and 399, with $(T_{\text{eff}}, \log g, v_t) = (4434 \text{ K}, 1.54, 1.5 \text{ km/s})$ and $(4419 \text{ K}, 1.8, 1.5 \text{ km/s})$. Carbon and nitrogen abundances were found to be of $[\text{C}/\text{Fe}]=0.0$, $[\text{N}/\text{Fe}]=+1.0$ for the CN-strong star 390 and $[\text{C}/\text{Fe}]=0.0$, $[\text{N}/\text{Fe}]=+0.50$ for the CN-weak star 399, assuming $[\text{O}/\text{Fe}]=+0.3$ in both cases. The difference in nitrogen abundances is clear, as shown in Fig. 15.

5. Discussion

The light elements C, N, O, Na, Mg and Al show variations in globular cluster stars. In M71 a bimodal distribution of CN-strong and CN-weak stars and an anticorrelation between CN and CH were first made evident by Smith & Norris (1982). For stars brighter than the Horizontal Branch (HB) level they showed that CN and CO are anticorrelated, and CN correlated with Na. Smith & Penny (1989) measured CN and CH based on the bandheads CN 3883 Å, CN 4215 Å and CH 4300 Å for a sample of HB stars in M71, and revealed an anticorrelation between CN and CH. CN-strong and CN-weak components were also revealed by Penny et al. (1992), who also showed an anticorrela-

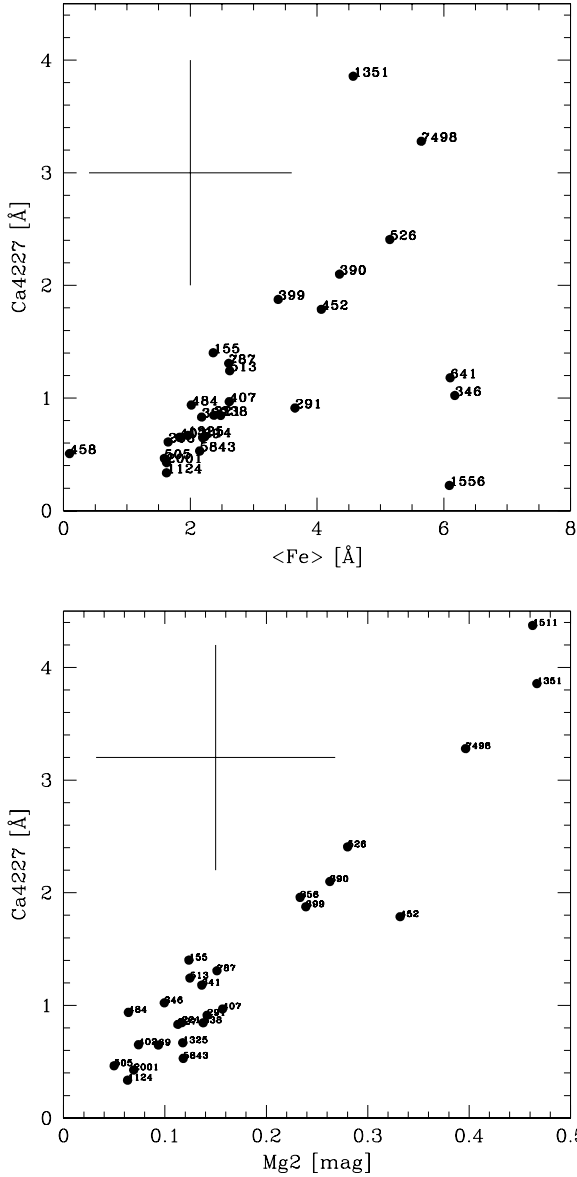


Fig. 11. *Upper panel:* Ca4227 vs. $\langle\text{Fe}\rangle$, and *Lower panel:* Ca4227 vs. Mg_2 . $\langle\text{Fe}\rangle = (\text{Fe}4383 + \text{Fe}5270 + \text{Fe}5335 + \text{Fe}5406)/4$.

tion CN-CH for subgiants in M71. A CN-bimodality and a CN-CH anticorrelation were also found for a sample of 79 MS stars in M71 by Cohen (1999). Briley et al. (2001) further derived CN and CH for 75 giants of M71 based on DDO photometric indices C(41-42) and C(42-45), and confirmed the C vs. N anticorrelation and the CN-strong and CN-weak components. Lee (2005) studied CN and CH band strength variations in 14 M71 giants showing clearly the CN bimodality, whereas the CN-CH anticorrelation is not clear in his analysis.

The behaviour of the CN and CH bands above is also reported for stars on the RGB and MS of 47 Tuc (see e.g. Norris & Freeman 1979; Norris, Freeman & Da Costa 1984; Cannon et al. 1998), another well studied Galactic globular cluster with metallicity close to that of M71 ($[\text{Fe}/\text{H}] = -0.67$, Alves-Brito et al. 2005). However, 47 Tuc is more massive than M 71, as well as more concentrated with a half-mass radius $r_h = 2.79$ arcmin

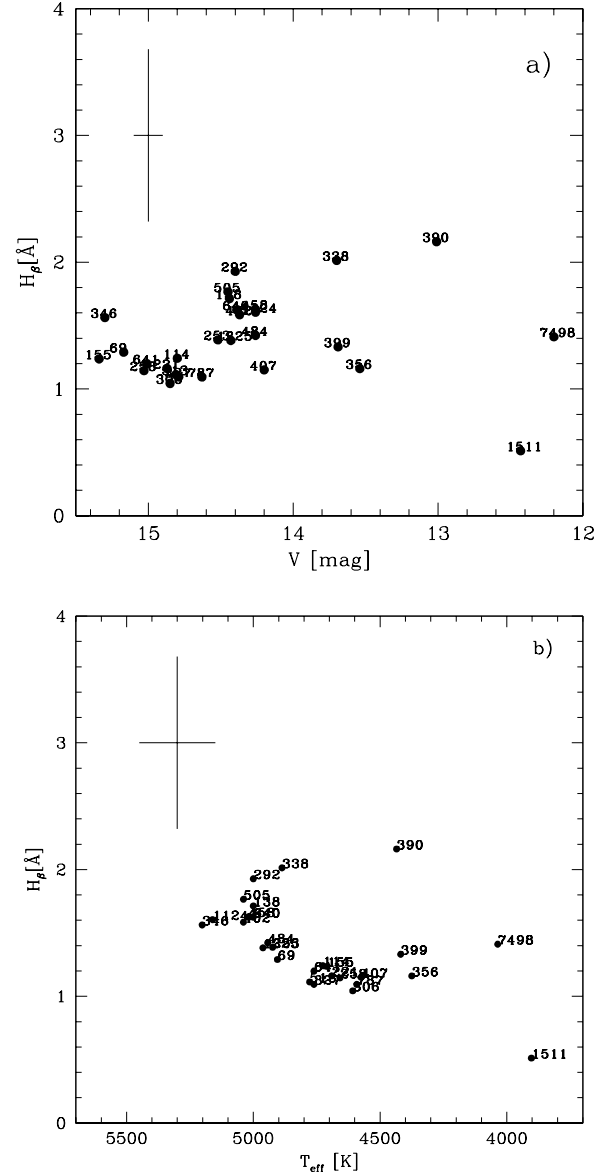


Fig. 12. *a):* H_β plotted against V, and *b):* H_β against T_{eff}

and concentration parameter $c=2.03$, whereas M 71 has $r_h = 1.65$ arcmin and $c=1.15$ (Harris 1996).

Based on the Cudworth (1985; 2006) star designations, it was possible to identify several stars in common with other spectroscopic studies (e.g. in Smith & Penny 1989; Penny et al. 1992; Lee 2005), which allows us to do a direct CN-CH band-strength comparison. The cross-check is possible for 15 out of 22 stars overlapping with our sample — 4 stars have no CN measurements in the literature, whereas we have no CN measurements for 3 other stars due to the position of the CCD gaps in their spectra. The comparison shows that 13 out of 15 stars present the same classification of CN-weak or CN-strong found in the present work, while 2 stars were found to present a different classification — stars 1-43 and 1-88 were previously classified as CN-strong. On the other hand, within a 1σ -uncertainty, those authors present the same CN values.

Regarding our CN-CH strength results, Fig. 7 illustrates the CN bimodality and CN-CH anticorrelations. Note, however, as discussed above, that 3 stars (IDs 1556, 1351 and 640) have inac-

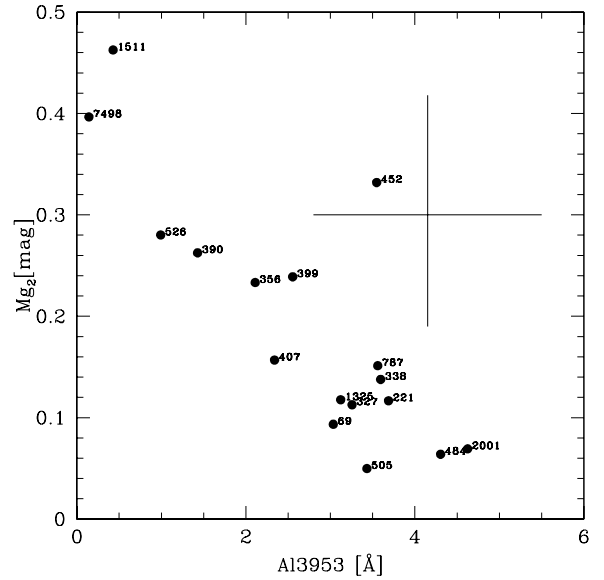
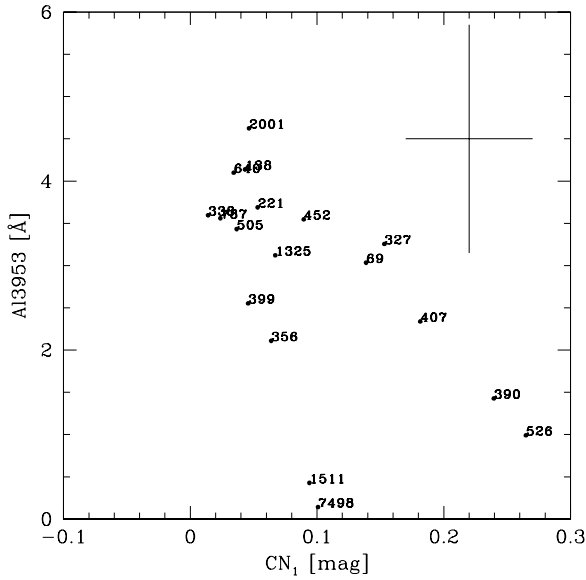
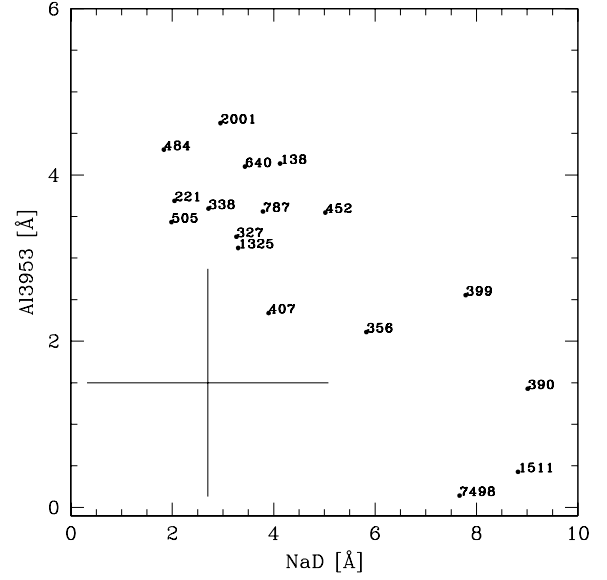
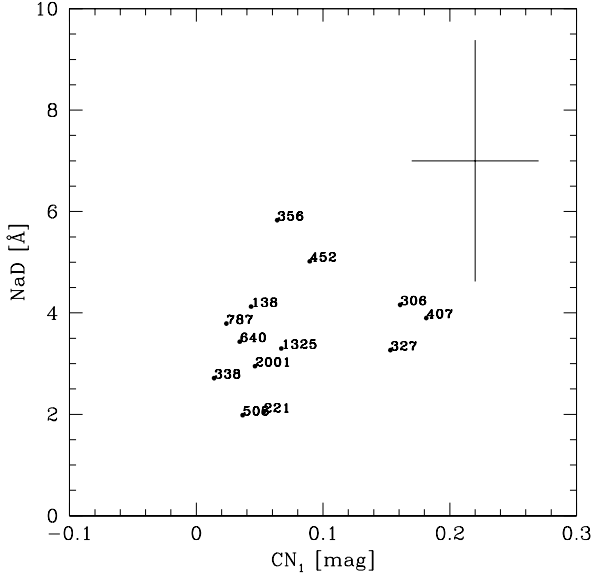


Fig. 13. NaD and Al3953 as a function of the CN index.

Fig. 14. *Top:* Al3953 vs. NaD. *Bottom:* Mg₂ vs. Al3953.

curate CN measurements due to the CCD gaps. Stars 2001, 458, and 505, which are classified as CN-weak, show lower CH values than other CN-weak stars. Even with some statistical outliers our CN-CH distribution has similar proportions as those given in Smith & Norris (1982).

Within the canonical framework of stellar structure and evolution of low-mass stars, the enhancement of nitrogen followed by the dredge-up of CN-processed material into the surface layers of such stars (Iben 1964; Charbonnel 1994). The present CN variations followed by an anticorrelation in the CH band confirm that an episode of deep mixing occurred in the M71 giants studied. On the other hand, the CN bimodality is better explained within a primordial pollution scenario. The mixing hypothesis does not explain the behaviour seen for the positive correlation between CN-Na and CN-Al, given that Na and Al are not produced during these mixing events.

Elements such as Al and Mg are produced by p-capture at higher temperatures (e.g. Langer & Hoffman 1995). As shown

in Fig. 14, there is a clear anticorrelation between Al3953 vs. NaD and Mg₂ indices. The Al-Mg anticorrelation seen in some globular cluster red giants is well explained by the enhanced extra mixing discussed in Denissenkov & Vandenberg (2003). Ramirez & Cohen (2002) reported a [Na/Fe]:[Al/Fe] correlation for their sample of M71 stars, however their results show a 2σ uncertainty (see their Fig. 13).

A scenario that appears plausible is that CNO-processed material in intermediate mass stars (IMS) on the AGB occurs early in the cluster's life, and their stellar winds are captured by low-mass stars (Gratton et al. 2004) or else by fast rotating massive stars (Decressin et al. 2007). Both the AGB or massive star early pollution possibilities are consistent with scenarios of self-enrichment proposed by Cayrel (1986), Parmentier et al. (1999), Parmentier & Gilmore (2001), Thoul et al. (2002), and Bekki et al. (2007). The latter developed a model of globular cluster formation in the central regions of low mass proto-galaxies embedded in dark matter halos. These proto-galaxies would retain the AGB ejecta and cause an "external pollution" of the globular

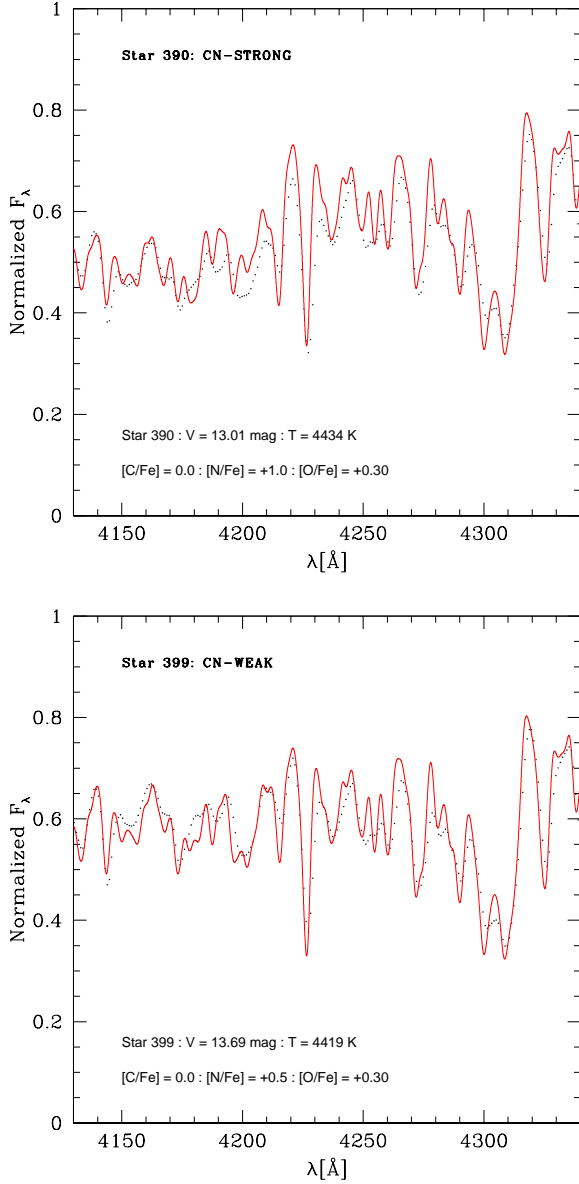


Fig. 15. Synthetic (solid line) and observed spectra (dotted line) in the region of CN and CH bands. *Upper panel:* Star 390 (CN-strong): T_{eff} , $\log g$, v_t) = (4434 K, 1.54, 1.5 km/s) computed for $[C/Fe]=0.0$, $[N/Fe]=+1.0$; *Lower panel:* Star 399 (CN-weak): (4419 K, 1.8, 1.5 km/s) computed for $[C/Fe]=0.0$, $[N/Fe]=+0.50$

cluster stars. This model can explain the C-N and Mg-Al anticorrelations, but shows a strong disagreement with the observed O-Na anticorrelation.

For the present sample, we found that CN and Na are correlated, while a CN-Al correlation does not appear. These CN-Na results imply a primordial explanation for abundance variations in M71.

6. Summary and conclusions

In M71 previous studies such that of Smith & Norris (1982) that first showed a bimodal distribution of CN-strong and CN-weak stars and an anticorrelation between CN and CH. This was followed by Smith & Penny (1989), Penny et al. (1992), Briley et

al. (2001), Cohen (1999), Ramirez et al. 2001, Ramírez & Cohen (2002), Boesgaard et al. (2005), and Lee (2005).

We measured CN, CH, Ca4277, iron and magnesium indicators, H_{β} , NaD and Al3953 spectral indices, from low-resolution spectra of 89 stars of the metal-rich globular cluster M71, observed with the Gemini Multi-Object Spectrograph (GMOS) at the Gemini-North telescope. CN and CH strengths were obtained for 89 stars, among which 33 giants. As expected from evolutionary mixing theories and additional extra-mixing (Iben 1964; Charbonnel 1994; Denissenkov & Vandenberg 2003), we find a CN-CH anticorrelation. We find CN-strong and CN-weak stars, with around 30% of CN-strong ones, similar to other clusters such as NGC 6752 with about 50%.

We confirm a CN-bimodality besides the CN-CH anticorrelation, a CN-Na correlation, and Al-Na and Mg₂-Al anticorrelation. The interpretation of CN bimodality is instead better understood in terms of primordial variations, and possible scenarios include an early enrichment by winds from intermediate mass stars in the AGB phase, and captured by low-mass stars, early in the cluster's life (Gratton et al. 2004 and references therein; Bekki et al. 2007) or early pollution by fast rotating massive stars (Decressin et al. 2007).

CN-strong and CN-weak bimodality is only seen in relatively metal-rich globular clusters, but not in all of them. Such behaviour is well studied in particular in 47 Tucanae, NGC 6752 and M4. Such abundance variations in metal-rich globular clusters is undoubtedly one of the most intricate challenges for the current theory of stellar evolution, and further observations with larger samples would be interesting.

Acknowledgements. AA acknowledges a FAPESP fellowship no. 04/00287-9. AA would like to thank the hospitality of the Department of Astronomy at the University of Virginia, during a visit in which part of this work was developed. Likewise, RPS would like to warmly thank the hospitality of the Astronomy Department at the University of São Paulo, during which much of this work was conceived. We are grateful to Professor Kyle Cudworth for cordially making his preliminary reduction of proper motions and photometry for M71 stars available to us. All observations were part of GEMINI Program GN-2002B-Q-42. This work is based on observations obtained at the Gemini Observatory, which is operated by the AURA, Inc., under a cooperative agreement with the NSF on behalf of the Gemini partnership: the NSF (United States), the PPARC (United Kingdom), the NRC (Canada), CONICYT (Chile), the ARC (Australia), CNPq (Brazil) and CONICET (Argentina)

References

- Alonso, A., Arribas, S., & Martínez-Roger, C. 1996, A&AS, 313, 873
- Alonso, A., Arribas, S., & Martínez-Roger, C. 1999, A&ASS, 140, 261
- Alonso, A., Arribas, S., & Martínez-Roger, C. 2001, A&A, 376, 1039
- Alves-Brito, A., Barbuy, B., Ortolani, S. et al. 2005, A&A, 435, 657
- Barbuy, B., Perrin, M.-N., Katz, D. et al. 2003, A&A, 404, 661
- Bekki, K., Campbell, S.W., Lattanzio, J.C., Norris, J.E. 2007, MNRAS, 377, 335
- Boesgaard, A. M., King, J. R., Cody, A. M., Stephens, A., Deliyannis, C. P. 2005, ApJ, 629, 832
- Briley, M. M., Smith, G. H., Claver, C. F. 2001, AJ, 122, 2561
- Cannon, R.D., Croke, B.F.W., Bell, R.A., Hesser, J.E., Stathakis, R.A. 1998, MNRAS, 298, 601
- Cardiel, N., Gorgas, J., Cenarro, J., Gonzalez, J. J. 1998, A&AS, 127, 597
- Castilho, B., Spite, F., Barbuy, B. et al. 1999, A&A, 345, 249
- Cayrel, R. 1986, A&A, 168, 81
- Cayrel, R., Perrin, M.-N., Buser, R., Barbuy, B., Coupry, M.-F. 1991, A&A, 247, 122
- Charbonnel, C. 1994, A&A, 282, 811
- Coelho, P., Barbuy, B., Meléndez, J., Schiavon, R., Castilho, B. 2005, A&A, 443, 735
- Cohen, J.G. 1980, ApJ, 241, 981
- Cohen, J.G., Gratton, R.G., Behr, B.B., & Carretta, E. 1999, ApJ, 523, 739
- Cohen, J. 1999, AJ, 117, 2434
- Cudworth, K. M. 1985, AJ, 90, 65
- Decressin, T., Meynet, G., Charbonnel, C., Prantzos, N., Ekström, S. 2007, A&A, 464, 1029

- Denissenkov, P.A., Vandenberg, D.A. 2003, *ApJ*, 593, 509
Dickens, R. J., Bell, R. A., Gustafsson, B. 1979, *ApJ*, 232, 428
Dinescu, D. I., Girard, T. M., van Altena, W. F. 1999, *AJ*, 117, 1792
Geffert, M.; Maintz, G. 2000, *A&AS*, 144, 227
Gratton, R., Sneden, C., Carretta, E. 2004, *ARA&A*, 42, 385
Grundahl, F., Stetson, P. B., Andersen, M. I. 2002, *A&A*, 395, 481
Gustafsson, B., Edvardsson, B., Eriksson, K., et al., 2008, *A&A*, in press
Harris, W.E. 1996, *ApJ*, 112, 1487
Hesser, J. E., Hartwick, F. D. A., McClure, R. D. 1977, *ApJS*, 33, 471
Hook, I. M., Jorgensen, I., Allington-Smith, J. R. et al. 2004, *PASP*, 116, 425
Iben, I. Jr., 1964, *ApJ*, 140, 1631
Kim, Y.-C., Demarque, P., Yi, S.K., Alexander, D. 2002, *ApJSS*, 143, 499
Kurucz, R. L. 1993, CD-ROM 23
Lee, Jae-Woo, Carney, B. W., Balachandran, S. C. 2004, *AJ*, 128, 2388
Lee, S.-G. 2005, *JKAS*, 38, 23
Kraft, R.P. 1994, *PASP*, 106, 553
Kraft, R.P., Ivans, I.I. 2003, *PASP*, 115., 143
Langer, G.E., Hoffman, R.D. 1995, *PASP*, 107, 1177
Leep, E. M., Wallerstein, G., Oke, J. B. 1987, *AJ*, 93, 338
Meissner, F., Weiss, A. 2006, *A&A*, 456, 1085
Norris, J., & Freeman, K.C. 1979, *ApJ*, 230, L179
Norris, J., Freeman, K.C. & Da Costa, G.S. 1984, *ApJ*, 277, 615
Parmentier, G., Jehin, E., Magain, P. et al. 1999, *A&A*, 352, 138
Parmentier, G., & Gilmore, G. 2001, *A&A*, 378, 97
Penny, A. J., Smith, G. H., Churchill, C. W. 1992, *MNRAS*, 257, 89
Prochaska, L.C., Rose, J.A., Schiavon, R.P. 2005, *AJ*, 130, 2666
Ramírez, S., Cohen, J.G., Buss, J., Briley, M.M. 2001, 122, 1429
Ramírez, S., Cohen, J. G. 2002, *AJ*, 123, 3277
Serven, J., Worthey, G., Briley, M.M. 2005, *ApJ*, 627, 754
Smith, G. H., 1987, *PASP*, 99, 67
Smith, G. H., Norris, J. 1982, *ApJ*, 254, 149
Smith, G. H., Penny, A. J. 1989, *AJ*, 97, 1397
Sneden, C., Kraft, R. P., Langer, G. E., Prosser, C. F., Shetrone, M. D. 1994, *AJ*, 107, 1773
Thoul, A., Jorissen, A., Goriely, S. et al. 2002, *A&A*, 383, 491
Thomas, D., Maraston, C., Bender, R. 2003, *MNRAS*, 343, 279
Vazdekis, A., Cenarro, A.J., Gorgas, J., Cardiel, N., Peletier, R.F. 2003, *MNRAS*, 340, 1317
Worthey, G., Faber, S. M., Gonzalez, J., Burstein, D. 1994, *ApJS*, 94, 687
Worthey, G., & Ottaviani, D.L. 1997, *ApJS*, 111, 377
Yong, D., Aoki, W., Lambert, D. L. 2006, *ApJ*, 638, 1018

Online Material

Table 1. Program stars : star identification (1, as given in the observation masks and Cudworth 1985;2006), coordinates J2000 (2)-(3), heliocentric radial velocities [km/s] (4), membership probabilities (5, provided by Cudworth 1985;2006), V magnitude (6), colours(7)-(8), bolometric magnitudes (9), gravities [dex](10), temperatures [K] (11).

ID	α	δ	v_r	P	V	B-V	(B-V) _o	Mbol	log g	T _{B-V}
(1)	(2)	(3)	(4)	(5)	(6)	(7)	(8)	(9)	(10)	(11)
155 : KC-141	298.4016	+18.75612	16.13	91	15.34	1.23	0.960	1.370	2.63	4709
138 : KC-127	298.3995	+18.79042	-8.10	90	14.44	1.07	0.800	0.602	2.43	5000
114 : KC-136	298.3962	+18.76293	16.62	93	14.80	1.22	0.950	0.839	2.43	4726
253 : KC-119	298.4147	+18.81320	123.03	95	14.52	1.11	0.840	0.650	2.42	4924
1468 [†] : ...	298.4188	+18.77991	-4.63	80	17.30	0.81	0.540	3.723	3.94	5799
367 : KC-343	298.4335	+18.79543	10.66	8	16.33	0.63	0.360	2.914	3.81	6500
327 : 1-73	298.4268	+18.78301	-31.76	96	14.79	1.20	0.930	0.846	2.44	4761
346 : KC-215	298.4298	+18.79586	37.87	93	15.30	0.97	0.700	1.539	2.88	5202
356 : 1-71	298.4318	+18.79003	-22.45	96	13.54	1.44	1.170	-0.627	1.71	4375
221 : 1-109	298.4103	+18.77245	23.54	96	14.87	1.24	0.970	0.891	2.44	4691
207 : 1639	298.4085	+18.79252	-4.87	95	17.00	0.75	0.480	3.477	3.90	6012
291 : 1-95	298.4206	+18.76555	16.01	96	13.30	1.29	1.020	-0.723	1.76	4608
306 : 1-75	298.4229	+18.79264	58.09	96	14.85	1.29	1.020	0.827	2.38	4608
751 : 1289	298.4129	+18.78219	-1.69	90	17.83	0.84	0.570	4.227	4.47	5705
3791 [†] : ...	298.4245	+18.79684	32.12	80	16.83	1.07	0.800	2.992	3.39	5000
1936 : 1280	298.4169	+18.77425	1.80	95	17.45	0.95	0.680	3.745	3.81	5366
390 : 1-66	298.4382	+18.77940	-14.50	81	13.01	1.40	1.130	-1.117	1.54	4435
1511 : 1-113	298.4403	+18.79596	-11.98	95	12.43	1.80	1.530	-2.222	0.87	3903
1124 : 1-88	298.4363	+18.76084	5.84	90	14.26	0.99	0.720	0.484	2.44	5161
69 : KC-202	298.4608	+18.81061	43.91	94	15.17	1.12	0.850	1.292	2.67	4905
7677 : 1346	298.4740	+18.79896	87.14	84	18.14	0.86	0.590	4.517	4.50	5634
51 [†] : ...	298.4469	+18.77311	-6.75	80	17.30	0.71	0.440	3.813	4.08	6165
488 [†] : ...	298.4532	+18.78136	-1.78	80	16.83	0.76	0.490	3.298	3.82	5976
7277 : KC-336	298.4665	+18.79440	17.59
1351 : 1-45	298.4507	+18.79796	39.18	94	12.36	1.76	1.490	-2.221	0.89	3950
573 : KC-196	298.4697	+18.79116	23.10	69	15.60	1.17	0.900	1.681	2.80	4814
505 : 1-34	298.4574	+18.78078	-107.0	95	14.45	1.05	0.780	0.628	2.46	5039
1556 : 1-46	298.4642	+18.79901	75.48	93	12.29	1.75	1.480	-2.275	0.88	3962
7498 : A4	298.4715	+18.77711	29.98	94	12.20	1.69	1.420	-2.271	0.91	4036
917 : KC-200	298.4624	+18.80419	62.65	86	15.53	1.30	1.030	1.498	2.64	4592
1796 : 1134	298.4556	+18.80151	86.97	91	18.69	0.83	0.560	5.097	4.45	5741
458 : 1-43	298.4485	+18.79111	27.59	94	14.26	1.06	0.790	0.430	2.37	5020
6761 : ...	298.4591	+18.77784	31.48
566 : KC-363	298.4681	+18.77355	-74.33	0	16.36	1.43	1.160	2.203	2.85	4390
439 : ...	298.4450	+18.77383	17.75
619 : 1355	298.4770	+18.79714	12.77	97	17.94	0.80	0.530	4.377	4.37	5852
1235 : 1670	298.4834	+18.79839	93.59	0	16.77	0.86	0.590	3.148	3.66	5635
640 : 1-48	298.4814	+18.79968	62.93	94	14.39	1.07	0.800	0.552	2.41	5000
122 : KC-303	298.3969	+18.77009	-30.64	0	16.01	0.81	0.540	2.433	3.42	5799
1035 : 1600	298.3999	+18.77520	-17.97	97	17.57	0.95	0.680	3.855	4.59	5336
787 : 1-59	298.4237	+18.80803	48.60	89	14.63	1.30	1.030	0.598	2.28	4592
292 : X	298.4207	+18.73372	-46.00	90	14.40	1.07	0.800	0.562	2.42	5000
258 : KC-152	298.4158	+18.73698	-2.72	85	15.03	1.26	0.990	1.034	2.48	4658
2984 [†] : ...	298.4104	+18.77345	-7.12	80	17.02	0.84	0.570	3.416	3.78	5699
328 [†] : ...	298.4270	+18.75018	-53.12	80	16.52	0.70	0.430	3.042	3.78	6205
1060 : ...	298.4140	+18.77067	-2.37	80
1294 : ...	298.4180	+18.78680	-5.85
792 [†] : ...	298.4254	+18.79479	-24.60	80	16.64	1.03	0.760	2.833	3.35	5079
13 : 1-79	298.4087	+18.77783	34.37	51	13.99	1.43	1.160	-0.167	1.90	4390
232 [†] : ...	298.4123	+18.77188	-11.50	80	16.84	1.06	0.790	3.010	3.40	5020
402 : 1-87	298.4396	+18.76128	-12.73	95	14.37	1.05	0.780	0.548	2.42	5039
4126 : ...	298.4290	+18.77043	-21.62
1633 : KC-374	298.4338	+18.78996	2.45	0	16.27	1.23	0.960	2.300	3.01	4709
2001 : 1-103	298.4317	+18.76827	-20.97	89	14.33	0.87	0.600	0.698	2.67	5604
1873 : ...	298.4356	+18.78181	-31.61
10387 : KC-267	298.4380	+18.77221	-34.8	39	15.69	0.44	0.170	2.443	3.87	7499

Table 1 – continued

ID	α	δ	v_r	P	V	B-V	(B-V) _o	Mbol	log g	T _{B-V}
(1)	(2)	(3)	(4)	(5)	(6)	(7)	(8)	(9)	(10)	(11)
1958 : ...	298.4417	+18.77365	-24.38
921 [†] : ...	298.4650	+18.77283	-4.46	80	16.53	0.72	0.450	3.034	3.76	6126
526 : 1-53	298.4607	+18.81613	40.67	95	12.97	1.61	1.340	-1.392	1.31	4138
484 : 1-55	298.4526	+18.80644	48.75	92	14.26	1.10	0.830	0.398	2.33	4943
6548 : 2071	298.4558	+18.80534	-5.19	90	19.85	1.05	0.780	6.027	4.65	5039
1181 : 1058	298.4628	+18.79180	-22.38	93	17.79	0.80	0.530	4.227	4.37	5852
1785 : 1-36	298.4463	+18.77901	-28.97	64	12.79	1.25	0.980	-1.197	1.60	4675
11860 : ...	298.4575	+18.80072	30.41
5871 : ...	298.4479	+18.79313	-57.30
6079 : ...	298.4502	+18.77050	-55.70
7299 : ...	298.4678	+18.80609	-63.31
7453 : ...	298.4694	+18.80521	36.21
1214 : 2084	298.4746	+18.80516	32.43	60	19.00	0.91	0.640	5.327	4.56	5465
951 : 2080	298.4727	+18.80355	48.11	82	18.08	0.77	0.500	4.546	4.31	5967
2154 : ...	298.4710	+18.78277	-6.90
1219 : 1356	298.4765	+18.79601	61.95	0	17.92	0.98	0.710	4.173	4.62	5243
1716 : ...	298.4827	+18.79184	-29.50
8009 : ...	298.4805	+18.79990	-139.8
654 : 1669	298.4843	+18.80037	52.82	0	17.26	1.28	1.010	3.246	3.35	4624
1926 : 1633	298.4001	+18.78803	-22.54	97	17.28	1.01	0.740	3.489	3.63	5120
3 : 1995	298.3983	+18.77371	3.43	98	16.92	1.11	0.840	3.050	3.38	4924
338 : 1-107	298.4283	+18.77441	0.02	90	13.70	1.13	0.860	-0.186	2.08	4887
391 : KC-234	298.4385	+18.76578	18.32	81	15.59	0.12	0.150
223 : KC-300	298.4105	+18.77746	5.90	26	16.11	1.12	0.850	2.232	3.05	4905
314 : ...	298.4240	+18.79783	113.38
1325 : 1-70	298.4343	+18.78580	18.25	92	14.43	1.09	0.820	0.576	2.41	4962
294 : 1308	298.4210	+18.79190	37.53	0	16.31	0.83	0.560	2.715	3.51	5732
4448 : ...	298.4327	+18.78299	0.11
10218 : ...	298.4360	+18.78151	-10.03
3915 : ...	298.4260	+18.78303	29.04
813 : ...	298.4306	+18.77201	5.21
266 : KC-223	298.4171	+18.77581	63.33	0	15.54	0.96	0.690	1.826	3.04	5338
256 : KC-224	298.4154	+18.76982	61.72	0	15.13	0.63	0.360	1.714	3.33	6500
1934 : ...	298.4136	+18.78399	7.47
206 : 1604	298.4084	+18.77378	48.45	83	16.83	0.87	0.600	3.198	3.67	5604
407 : 1-65	298.4402	+18.78101	4.68	80	14.20	1.31	1.040	0.159	2.10	4575
1693 : ...	298.4683	+18.80594	51.17
1818 : ...	298.4662	+18.80561	81.33
6868 : ...	298.4617	+18.80363	84.90
1210 : 1342	298.4741	+18.80269	72.68	92	18.50	0.83	0.560	4.907	4.45	5741
2013 : ...	298.4565	+18.80247	120.85
1161 : ...	298.4523	+18.80226	72.23
6786 : ...	298.4601	+18.73407	-11.68
12299 : ...	298.4637	+18.78218	12.36
888 [†] : ...	298.4543	+18.78301	3.27	80	17.39	1.37	1.100	3.293	3.32	4481
7505 : ...	298.4702	+18.79745	60.95
7573 : ...	298.4724	+18.79126	93.07
452 : 1-21	298.4475	+18.76873	4.58	95	13.02	1.49	1.220	-1.200	1.45	4302
10927 : ...	298.4456	+18.77864	219.80
5964 : ...	298.4495	+18.77822	11.88
1897 : ...	298.4584	+18.77371	-2.35
613 : 1378	298.4761	+18.78647	27.41	97	17.57	0.89	0.620	3.917	4.53	5531
641 : KC-191	298.4816	+18.79488	25.35	85	15.01	1.20	0.930	1.066	2.53	4761
651 : KC-170	298.4838	+18.75471	-15.25	92	15.57	1.14	0.870	1.676	2.82	4868
720 : KC-125	298.4006	+18.79778	57.44	38	15.32	1.12	0.850	1.442	2.73	4905
4 : 2021	298.3983	+18.78664	-31.06	99	17.59	0.96	0.690	3.865	4.60	5305
399 : 1-81	298.4392	+18.77778	-0.78	95	13.69	1.41	1.140	-0.447	1.80	4419
1282 : KC-298	298.4108	+18.79258	-20.66	8	16.15	1.22	0.950	2.189	2.97	4726
1081 : ...	298.4221	+18.77992	-2.77

Table 1 – continued

ID	α	δ	v_r	P	V	B-V	$(B-V)_o$	Mbol	log g	T_{B-v}
(1)	(2)	(3)	(4)	(5)	(6)	(7)	(8)	(9)	(10)	(11)
829 : KC-265	298.4352	+18.77724	-7.32	70	15.50	1.25	0.980	1.513	2.68	4675
4482 : ...	298.4329	+18.79019	-21.82
1486 : ...	298.4293	+18.77786	-16.28
3909 : ...	298.4273	+18.78753	-17.13
1087 : ...	298.4247	+18.77539	-7.65
387 : ...	298.4374	+18.79451	-9.97
778 : ...	298.4201	+18.78474	-22.07
2045 : ...	298.4178	+18.78361	-26.96
1292 [†] : ...	298.4159	+18.77535	-10.03	80	17.31	1.19	0.920	3.374	3.46	4778
242 : 1281	298.4135	+18.77435	21.63	94	17.56	0.99	0.720	3.803	4.62	5213
212 : KC-128	298.4089	+18.78764	-21.42	0	15.19	1.37	1.100	1.093	2.44	4481
5412 : ...	298.4417	+18.78268	-11.30
574 : ...	298.4698	+18.80458	66.35
78 : 1341	298.4731	+18.80265	51.13	96	18.08	0.79	0.520	4.526	4.34	5890
1561 : ...	298.4658	+18.80221	55.75
1894 : ...	298.4537	+18.80117	81.02
881 : KC-252	298.4516	+18.78288	-19.77	0	15.38	0.69	0.420	1.911	3.34	6245
7014 : ...	298.4625	+18.78173	-22.03
11907 : ...	298.4568	+18.79274	-34.30
523 : ...	298.4605	+18.78475	-11.23
2229 : ...	298.4750	+18.78421	14.80
2153 : ...	298.4674	+18.79044	1.29
513 : 1-11	298.4587	+18.76193	1.72	87	14.81	1.19	0.920	0.874	2.46	4778
5843 : 1-42	298.4474	+18.78542	-236.7	94	14.22	1.02	0.750	0.421	2.39	5099
11331 : ...	298.4495	+18.77523	-18.35
1144 : ...	298.4455	+18.78746	-6.37
1815 : ...	298.4642	+18.77378	-12.25
616 : 1158	298.4767	+18.77737	-4.03	99	17.50	0.89	0.620	3.850	3.91	5542
8076 : ...	298.4831	+18.79152	-8.45
1409 : ...	298.4810	+18.79049	-5.78

Table 3. Selected spectral indices and uncertainties

ID	CN ₁	σ CN ₁	CN ₂	σ CN ₂	Ca4227	σ Ca4227	G4300	σ G4300	Fe4383	σ Fe4383
(1)	(2)	(3)	(4)	(5)	(6)	(7)	(8)	(9)	(10)	(11)
155	1.40243	0.06233	6.52152	0.10159	4.20713	0.14444
138	0.04322	0.00209	0.07336	0.00244	0.57001	0.03885	5.92503	0.05891
114	0.16148	0.00286	0.20422	0.00334	0.65743	0.05216	5.96941	0.07767	3.61326	0.11121
253	0.00931	0.00229	0.03234	0.00269	0.61062	0.04255	6.61777	0.06490	2.60329	0.09691
1468	-0.05119	0.00791	-0.02598	0.00911	1.20442	0.13622	3.78093	0.23611	1.77363	0.32466
367	-0.11786	0.00402	-0.07367	0.00460	0.22357	0.07454	9.08490	0.15210	0.83578	0.18196
327	0.15312	0.00276	0.19179	0.00323	0.83128	0.05027	6.08654	0.07403	3.37153	0.10663
346	-0.03214	0.00320	-0.00845	0.00374	1.02249	0.05736	2.97693	0.13212
356	0.06381	0.00178	0.11698	0.00207	1.95910	0.02910	6.39225	0.04704
221	0.05313	0.00288	0.08605	0.00337	0.84705	0.05208	6.44599	0.07955	4.06963	0.11329
207	-0.09300	0.00632	-0.04139	0.00723	0.33972	0.11780	0.85977	0.20239
291	0.22158	0.00150	0.27198	0.00175	0.91187	0.02664	6.88402	0.03843	4.58861	0.05606
306	0.16083	0.00292	0.18856	0.00342	0.69245	0.05200	6.14833	0.07913
751	-0.04367	0.01090	-0.00666	0.01261	3.92085	0.32847	1.47634	0.44154
3791	-0.12458	0.00753	-0.10661	0.00893	0.76429	0.12619	3.96273	0.26997
1936	-0.04689	0.00953	-0.01048	0.01100	0.54118	0.17870	4.96705	0.27965	1.76341	0.39538
390	0.23949	0.00155	0.30867	0.00180	2.09909	0.02481	6.18513	0.03913	5.44020	0.05304
1511	0.09395	0.00150	0.18146	0.00173	4.37277	0.01886	7.48770	0.04667
1124	0.06381	0.00191	0.09721	0.00223	0.33596	0.03605	5.94786	0.05428	2.55372	0.08127
69	0.13869	0.00331	0.17676	0.00388	0.64753	0.06135	5.97267	0.09010	3.79636	0.12857
7677	-0.16205	0.01560	-0.10893	0.01828	3.00907	0.41338	0.16882	0.56815
51	-0.11096	0.00500	-0.07487	0.00573	0.43956	0.09148	0.12812	0.16555	0.69300	0.22525
488	-0.11935	0.00471	-0.08912	0.00539	0.45728	0.08761	0.04795	0.15723	-0.34789	0.21842
7277	0.08145	0.00807	0.12601	0.00939	0.55541	0.14618	3.42389	0.31066
1351	-0.05832	0.00184	0.02940	0.00225	3.85582	0.01897	6.14184	0.04448
573	0.10763	0.00404	0.14294	0.00472	0.59885	0.07394	6.17838	0.10958
505	0.03659	0.00196	0.06304	0.00229	0.46435	0.03698	5.15907	0.05645	2.40308	0.08498
1556	-0.01914	0.00154	0.05687	0.00182	0.22444	0.05328	5.65096	0.03468	6.67513	0.04359
7498	0.10080	0.00125	0.17497	0.00144	3.27895	0.01755	4.67087	0.03349	6.25388	0.04099
917	0.27506	0.00421	0.30047	0.00504	1.26933	0.06688	6.48284	0.10694	4.26310	0.15185
1796	-0.11522	0.01992	-0.04566	0.02258	-0.59468	0.39629	2.63782	0.59020	4.59379	0.74652
458	0.05273	0.00192	0.07980	0.00225	0.50643	0.03598	5.32540	0.05504
6761	-0.01236	0.00495	0.00076	0.00581	1.04621	0.08799	5.31722	0.14631	2.94120	0.20350
566	0.30405	0.00956	0.35146	0.01113	1.94359	0.15123	6.34852	0.22361	8.89226	0.27095
439	0.00500	0.00544	0.04180	0.00638	2.29010	0.08608	5.69465	0.15290	6.57911	0.19907
619	-0.28551	0.01437	-0.26438	0.01701	0.86945	0.22357
1235	-0.22732	0.00721	-0.20723	0.00878	3.81334	0.17853	3.68435	0.24416
640	0.03427	0.00206	0.06479	0.00240	6.10977	0.05766	2.43395	0.08702
122	-0.05273	0.00420	-0.01804	0.00488	0.98398	0.07342	5.08607	0.12400	3.63184	0.17351
1035	-0.02359	0.01100	0.00633	0.01277	1.24578	0.18844	6.25670	0.30724	2.31461	0.43753
787	0.02371	0.00272	0.05826	0.00319	1.30720	0.04702	6.68840	0.07455	4.48230	0.10477
292
258
2984	-0.14430	0.00606	-0.08624	0.00685	0.43245	0.10648	0.31503	0.26645
328
1060	-0.04419	0.00658	-0.02330	0.00766	1.01418	0.11492	5.22738	0.19162	4.25402	0.25825
1294	-0.08150	0.00653	-0.05349	0.00753	0.76681	0.11435	3.83046	0.19669	3.35720	0.26601
792	0.09121	0.00629	0.12761	0.00733	0.54454	0.11504	3.26673	0.24300
13	0.33752	0.00245	0.38891	0.00287	2.20860	0.03768	6.56970	0.06089	8.60797	0.07663
232	0.06822	0.00707	0.09758	0.00826	0.68816	0.12664	6.07985	0.19627	3.19207	0.27471
402	0.00322	0.00201	0.03490	0.00236	0.65140	0.03694	6.62719	0.05728	3.13987	0.08479
4126	-0.06555	0.00987	-0.03858	0.01148	0.52887	0.17753	5.21713	0.28995	2.85185	0.38755
1633	0.03326	0.00600	0.07421	0.00697	0.94044	0.10219	4.80354	0.17021
2001	0.04630	0.00192	0.08012	0.00224	0.42717	0.03574	5.42182	0.05505	2.65181	0.08199
1873	0.07294	0.00462	0.11101	0.00540	0.74710	0.08374	5.98203	0.12879	3.46350	0.18147
10387	-0.04575	0.00919	-0.00573	0.01066	0.98490	0.16133	4.32741	0.27375	1.49539	0.37778
1958	-0.00999	0.00909	0.00437	0.01062	1.27912	0.15579	5.13404	0.26472	3.77817	0.35257
921	-0.13095	0.00475	-0.08016	0.00541	0.42099	0.08537	0.35964	0.15617	0.96461	0.21184

Table 3 – continued

ID	CN ₁	σ CN ₁	CN ₂	σ CN ₂	Ca4227	σ Ca4227	G4300	σ G4300	Fe4383	σ Fe4383
(1)	(2)	(3)	(4)	(5)	(6)	(7)	(8)	(9)	(10)	(11)
526	0.26481	0.00159	0.34027	0.00184	2.40689	0.02432	5.83910	0.04022	6.13915	0.05277
484	-0.47637	0.00243	-0.56421	0.00258	0.93837	0.03691	6.77858	0.05744	3.32696	0.08513
6548	-0.20698	0.08652	-0.06987	0.09158	0.02042	1.63150	11.91655	1.72551	6.94459	2.48834
1181	-0.05243	0.01017	-0.03674	0.01178	0.29992	0.18605	3.08939	0.31174
1785	0.07411	0.00135	0.12348	0.00157	2.04942	0.02106	6.33864	0.03625	4.90075	0.05023
11860	-0.03443	0.01391	-0.01236	0.01593	4.03324	0.40083	0.47772	0.57048
5871	-0.02782	0.01694	0.00359	0.01955	1.20888	0.30302	5.24213	0.47669
6079	-0.03227	0.00823	0.00465	0.00951	0.36602	0.14961	4.34266	0.24242	2.00205	0.33880
7299	-0.47582	0.02691	-0.21301	0.02678	-0.64381	0.44082	2.80661	0.69593	2.92516	0.86582
7453	-0.15532	0.02188	0.01301	0.02415	-0.18546	0.38075	4.69649	0.58547	1.52503	0.78843
1214	-0.07199	0.03844	0.14304	0.04279	2.38127	0.57191	4.32146	1.08741	3.67873	1.27111
951	0.87056	0.01535	0.91164	0.01855	0.55276	0.22763	4.29836	0.36736	3.39299	0.49865
2154	-0.05583	0.01052	-0.02170	0.01215	0.68669	0.18524	3.49960	0.31683	1.77232	0.43230
1219	-0.10577	0.01253	-0.06338	0.01435	0.49662	0.22758	3.43794	0.48384
1716	-0.13661	0.00631	-0.09596	0.00719	0.23661	0.11408	-0.15670	0.20915
8009	0.03526	0.00224	0.07428	0.00263	5.97122	0.06453	1.87757	0.09987
654	0.18035	0.01310	0.22882	0.01521	6.93690	0.32121	7.83077	0.39086
1926	-0.04897	0.00966	-0.00731	0.01119	1.21283	0.16833	5.84349	0.27408
3	-0.02560	0.00823	0.00403	0.00958	1.49943	0.13918	6.89493	0.22869	4.09773	0.31600
338	0.01406	0.00154	0.04509	0.00180	0.84549	0.02772	6.83656	0.04287	3.83291	0.06323
391	-0.17651	0.00202	-0.12477	0.00232	0.07480	0.03770	-1.95439	0.07245	-0.24489	0.09981
223	-0.03701	0.00518	-0.01518	0.00606	1.33425	0.08930	6.16913	0.14783	4.14466	0.20541
314	-0.06419	0.00442	-0.03510	0.00551	0.63777	0.06511	-5.31927	0.17046	5.54108	0.13067
1325	0.06705	0.00221	0.10230	0.00258	0.66800	0.04039	6.21177	0.06147	3.24518	0.08977
294	-0.09128	0.00431	-0.05734	0.00497	0.79088	0.07661	2.72706	0.13396
4448	-0.04674	0.00962	-0.02689	0.01111	0.69301	0.16902	5.76952	0.26768	4.32254	0.36258
10218	-0.07782	0.00933	-0.06129	0.01091	1.52458	0.15989	6.33231	0.27135	3.50866	0.37583
3915	-0.03427	0.00753	-0.00254	0.00873	0.81765	0.13165	4.61150	0.22174	3.62914	0.29753
813	-0.05018	0.00941	-0.02849	0.01090	0.85558	0.16762	5.60970	0.27368	1.34962	0.39138
266	0.01584	0.00355	0.04366	0.00417	1.12150	0.06188	6.17802	0.10090	5.27360	0.13822
256	-0.10115	0.00225	-0.05742	0.00259	0.46543	0.04089	1.27847	0.07316	0.84223	0.10319
1934	-0.03054	0.01361	0.00659	0.01574	0.87601	0.23547	5.99504	0.37867	3.59718	0.50286
206	-0.05680	0.00588	-0.01722	0.00679	0.70195	0.10422	3.36285	0.17957	2.05268	0.25121
407	0.18144	0.00221	0.23267	0.00258	0.96804	0.03931	6.13439	0.05880	4.30138	0.08311
1693	-0.47713	0.02065	-0.05334	0.02048	0.89438	0.30345	4.56961	0.51913	0.27190	0.70931
1818	-0.36121	0.01282	-0.03056	0.01330	0.50417	0.20503	3.65259	0.34537	1.34578	0.47705
6868	0.91228	0.00644	0.92786	0.00797	0.97512	0.09404	6.20008	0.15204	3.91007	0.21252
1210	0.65785	0.02053	0.68796	0.02464	0.91656	0.30387	4.07550	0.53275	1.32334	0.72966
2013	0.34051	0.02131	0.37325	0.02540	1.09970	0.33150	3.14698	0.58426	4.16090	0.71026
1161	0.08280	0.01091	0.11446	0.01263	0.25457	0.19455	3.52170	0.31192	1.42484	0.43431
6786
12299	-0.07973	0.01201	-0.04176	0.01378	0.84948	0.21222	2.92355	0.36646	0.57294	0.51187
888	-0.03084	0.00837	-0.00614	0.00976	1.30186	0.14423	6.23319	0.23699	3.20632	0.32733
7505	-0.25368	0.02663	-0.22219	0.03254	0.96518	0.37183	3.56761	0.81444
7573	-0.11943	0.00765	-0.08628	0.00876	0.79454	0.13432	2.51309	0.23491
452	0.08950	0.00139	0.14386	0.00162	1.78711	0.02295	7.01376	0.03626	5.66200	0.05088
10927	0.01186	0.00224	0.04661	0.00262	0.88830	0.04067	6.49662	0.06284	3.43493	0.09240
5964	-0.07156	0.00758	-0.04183	0.00874	0.52348	0.13665	3.78778	0.22987	1.98014	0.32230
1897	0.10768	0.00286	0.14716	0.00336	0.66077	0.05207	6.78805	0.07778	4.07202	0.11229
613	-0.04641	0.01029	-0.02407	0.01196	0.96931	0.18284	4.88181	0.30334	2.18303	0.41935
641	0.00364	0.00305	0.03812	0.00357	1.18037	0.05298	-1.41249	0.18450	4.14242	0.12083
651	1.03547	0.07039	6.31482	0.11376	4.30139	0.15996
720	-0.13785	0.00441	-0.11155	0.00548	0.74089	0.06422	1.89742	0.12369	4.84172	0.13704
4	-0.00156	0.01041	0.02518	0.01209	0.39857	0.19199	5.60566	0.29540	3.12601	0.40588
399	0.04562	0.00178	0.09435	0.00208	1.87527	0.02910	6.61648	0.04830	5.00537	0.06630
1282	0.06081	0.00595	0.09594	0.00694	0.64202	0.10821	5.74375	0.16551
1081	0.08356	0.00902	0.12738	0.01054	0.40182	0.16364	5.85833	0.25165	3.55485	0.34161
829	0.01706	0.00370	0.04976	0.00434	0.88499	0.06639	6.55853	0.10393	3.93711	0.14846
4482	-0.05420	0.00868	-0.01129	0.01003	0.40235	0.15846	4.03163	0.26355	12.87503	0.33871

Table 3 – continued

ID	CN ₁	σ CN ₁	CN ₂	σ CN ₂	Ca4227	σ Ca4227	G4300	σ G4300	Fe4383	σ Fe4383
(1)	(2)	(3)	(4)	(5)	(6)	(7)	(8)	(9)	(10)	(11)
1486	-0.02960	0.00616	-0.00929	0.00721	0.98922	0.10984	6.09164	0.17795	3.34564	0.25024
3909	-0.03718	0.01094	-0.01604	0.01276	1.34264	0.18482	6.19278	0.31139	4.52232	0.41026
1087	-0.03726	0.00854	-0.02204	0.00998	1.06079	0.14747	5.41860	0.25044	3.34544	0.33815
387	-0.02069	0.00983	0.00733	0.01135	0.30317	0.17918	2.00333	0.40705
778	-0.05408	0.00809	-0.02809	0.00942	0.87503	0.14206	6.25716	0.22945	3.22521	0.31751
2045	-0.02555	0.00873	0.00923	0.01013	0.71226	0.15574	4.90365	0.25730	2.94711	0.35295
1292	0.05908	0.00881	0.08318	0.01027	0.66925	0.15659	5.30523	0.24976	3.09910	0.33919
242	-0.03314	0.01028	-0.04201	0.01210	-0.08970	0.19387	-1.32111	0.34966	-2.46920	0.43904
212	0.32203	0.00430	0.36940	0.00504	1.75513	0.06757	6.36811	0.10780	2.63306	0.15386
5412	-0.02477	0.00416	0.00186	0.00488	1.22956	0.07329	6.54181	0.11903	3.79534	0.16883
574	-0.03900	0.01043	-0.01161	0.01205	0.79684	0.17904	3.68958	0.30908	1.10257	0.43295
78	0.59898	0.01486	0.64246	0.01777	0.69810	0.22874	2.62810	0.39217	2.19301	0.52092
1561	0.14645	0.01022	0.16950	0.01205	0.97467	0.17233	5.39462	0.28533	2.85040	0.39194
1894	-0.06735	0.01336	-0.01400	0.01535	-0.50545	0.29880	4.20661	0.39315	1.57301	0.55144
881	-0.09442	0.00272	-0.06150	0.00316	0.74754	0.04900	3.05938	0.08590	2.17886	0.12137
7014	-0.08444	0.00977	-0.06065	0.01129	0.66799	0.17541	4.31525	0.29040	1.99912	0.40444
11907	-0.05077	0.01776	-0.03992	0.02030	0.65460	0.32048	2.60527	0.52215
523	-0.05529	0.00580	-0.03232	0.00677	0.78350	0.10449	5.52678	0.17170	2.27632	0.24667
2229	-0.03723	0.02017	-0.07712	0.02343	0.80141	0.34639	2.40803	0.61903	1.39969	0.79086
2153	-0.06382	0.01067	-0.04757	0.01232	0.36437	0.19238	1.93115	0.33241
513	-0.00838	0.00270	0.02281	0.00317	1.24215	0.04679	6.60797	0.07623	4.45550	0.10726
5843	0.00490	0.00216	0.04651	0.00253	0.53005	0.03981	6.34083	0.06206	3.13525	0.09067
11331	-0.07463	0.01154	-0.03743	0.01316	0.46931	0.20410	1.90226	0.36061	1.69964	0.48202
1144	-0.06654	0.00631	-0.04187	0.00734	0.55505	0.11493	3.58999	0.19515	1.04941	0.27398
1815	-0.03459	0.00859	0.00321	0.00995	0.68996	0.15462	3.67910	0.26479	2.20097	0.36367
616	-0.03597	0.00954	-0.00280	0.01104	0.37572	0.17640	4.65663	0.27798	2.23361	0.39137
8076	-0.02301	0.01376	-0.00136	0.01594	1.00646	0.23899	5.91934	0.39427
1409	-0.06957	0.01594	-0.04636	0.01848	1.24008	0.27302	4.27523	0.47819

Table 4. Selected spectral indices and uncertainties.

ID	H β	σ H β	Mg $_1$	σ Mg $_1$	Mg $_2$	σ Mg $_2$	Mgb	σ Mgb	Fe5270	σ Fe5270
(1)	(2)	(3)	(4)	(5)	(6)	(7)	(8)	(9)	(10)	(11)
155	1.23728	0.05199	0.08470	0.00103	0.12360	0.00118	2.68898	0.04557	2.22092	0.04909
138	1.71328	0.03203	-0.12243	0.00070	-0.11571	0.00082	1.48913	0.02953	1.77792	0.03179
114	1.24208	0.04006	-0.15352	0.00085	-0.00161	0.00100	2.54644	0.03525	2.30571	0.03787
253	1.38706	0.03437	-0.20548	0.00073	-0.07328	0.00086	1.51620	0.03057	1.78977	0.03300
1468	2.65934	0.11462	-0.00489	0.00239	0.05761	0.00277	1.93860	0.10763	1.13950	0.12007
367	4.51381	0.06618	-0.01103	0.00146	0.03080	0.00170	0.83520	0.06797
327	1.09457	0.03862	0.02683	0.00076	0.11273	0.00088	2.63517	0.03389	2.26211	0.03668
346	1.56316	0.04784	0.01315	0.00095	0.09936	0.00110	2.33412	0.04280
356	1.16060	0.02257	0.05118	0.00044	0.23330	0.00051	5.80145	0.01837	5.23928	0.01947
221	1.16138	0.04050	0.03127	0.00079	0.11667	0.00092	2.51160	0.03568	2.33846	0.03833
207	3.56054	0.09910	-0.15108	0.00235	-0.16891	0.00276	1.31818	0.09635	-1.42167	0.11879
291	-0.03089	0.00040	0.14155	0.00047	5.58068	0.01603	4.32468	0.01797
306	1.04347	0.04056	-0.14163	0.00088	-0.11593	0.00104	2.51789	0.03535	0.49334	0.04177
751	2.30296	0.14787	-0.01354	0.00298	0.06002	0.00347	2.08246	0.13429	1.06271	0.14987
3791	1.44281	0.09524	0.01762	0.00186	0.12448	0.00216	2.91656	0.08285
1936	2.17713	0.13621	0.00159	0.00277	0.06561	0.00321	2.30901	0.12321	1.38998	0.13753
390	2.16206	0.01801	0.07967	0.00036	0.26260	0.00042	5.87791	0.01494	4.67364	0.01597
1511	0.51285	0.01603	0.16339	0.00029	0.46267	0.00034	9.33388	0.01097
1124	1.60465	0.03012	-0.00090	0.00061	0.06318	0.00070	1.38917	0.02795	1.67990	0.03005
69	1.29073	0.04644	-0.01062	0.00091	0.09353	0.00105	2.53874	0.04057	2.11044	0.04414
7677	2.53599	0.18895	0.01715	0.00383	0.29555	0.00464	0.46097	0.19353
51	4.17705	0.08207	-0.01638	0.00181	0.02145	0.00210	0.70527	0.08436	0.87296	0.09253
488	4.67647	0.07682	-0.01882	0.00172	0.01528	0.00200	0.65243	0.08007	0.49508	0.08909
7277	1.26708	0.11188	0.02544	0.00221	0.12725	0.00257	2.76926	0.09961	-1.94239	0.15577
1351	3.44805	0.01349	0.13626	0.00027	0.46681	0.00032	7.98301	0.01116	4.47050	0.01307
573	1.33233	0.05689	-0.14624	0.00126	-0.12155	0.00149	2.73845	0.05011	2.06642	0.05484
505	1.76574	0.03115	-0.00179	0.00063	0.04987	0.00073	1.35788	0.02908	1.63092	0.03116
1556	2.09879	0.01436	0.10862	0.00027	0.83700	0.00000	1.00676	0.00000	6.77846	0.01171
7498	1.41136	0.01379	0.09837	0.00026	0.39654	0.00031	9.42370	0.00970	6.78767	0.01087
917	1.27861	0.05491	0.38326	0.00118	0.10001	0.00124	2.89567	0.04731	2.04703	0.05199
1796	2.85003	0.24088	0.01463	0.00492	0.26408	0.00593	1.93956	0.23596
458	1.62785	0.02992	-0.16368	0.00067	-0.17168	0.00079	1.52897	0.02749	1.75849	0.02974
6761	1.29554	0.07244	0.01929	0.00143	0.12197	0.00166	3.07572	0.06320	1.98001	0.06970
566	1.19253	0.09369	0.13259	0.00178	0.27367	0.00207	4.31677	0.07882	4.29264	0.08006
439	1.58764	0.07617	0.05857	0.00155	0.25694	0.00182	5.40309	0.06666	4.03782	0.07239
619	2.84987	0.16601	0.00785	0.00336	0.07498	0.00390	1.69603	0.15437
1235	3.39252	0.09002	0.00456	0.00190	0.10344	0.00221	1.88367	0.09305
640	1.62410	0.03179	0.01277	0.00063	0.77913	0.00083	1.84062	0.03095
122	3.24323	0.06420	-0.00102	0.00136	0.10073	0.00159	2.58008	0.06119	2.29205	0.06691
1035	2.23247	0.14782	-0.00871	0.00297	0.06649	0.00345	2.43341	0.13191	1.24939	0.14682
787	1.09383	0.03680	0.00699	0.00070	0.15129	0.00082	3.97123	0.03041	2.61899	0.03365
292	1.92752	0.03211	0.01005	0.00065	0.07958	0.00075	1.30156	0.03006	1.69910	0.03202
258	1.14495	0.04660	0.02982	0.00090	0.12110	0.00104	2.73249	0.04020	2.19098	0.04347
2984	4.76758	0.09328	-0.01603	0.00207	0.02870	0.00240	1.06460	0.09508	0.97310	0.10535
328	6.10282	0.06981	-0.03779	0.00161	0.64557	0.00211	0.47747	0.08361
1060	2.70831	0.09482	0.01935	0.00198	0.13473	0.00231	3.18005	0.08793	2.66695	0.09571
1294	3.51839	0.09689	-0.01609	0.00206	0.06787	0.00240	1.99589	0.09330	1.96330	0.10188
792	1.23244	0.08777	0.02261	0.00171	0.12557	0.00199	2.88605	0.07623
13	1.65260	0.02839	0.10058	0.00056	0.31425	0.00065	6.30576	0.02327	5.53427	0.02447
232	1.35785	0.09753	0.01068	0.00193	0.10319	0.00225	2.79735	0.08584	1.91094	0.09458
402	1.58513	0.03117	0.01555	0.00063	0.07392	0.00073	1.52584	0.02889	1.84671	0.03105
4126	1.75579	0.13275	0.00465	0.00266	0.10422	0.00310	2.91400	0.11802	1.91177	0.13038
1633	1.61262	0.07893	0.05786	0.00156	0.17183	0.00182	3.14839	0.07013	2.60730	0.07467
2001	0.00098	0.00062	0.06921	0.00072	1.62211	0.02820	1.68697	0.03051
1873	1.25060	0.06666	0.00825	0.00132	0.10383	0.00153	2.65167	0.05896	1.90914	0.06482
10387	1.70260	0.13353	-0.00494	0.00268	0.07419	0.00311	2.33884	0.11980	1.07864	0.13392
1958	1.46306	0.12321	0.01189	0.00241	0.11348	0.00281	3.35021	0.10536	2.03251	0.11721
921	5.62486	0.07594	-0.01133	0.00175	0.03775	0.00203	0.80619	0.08143	1.25727	0.08861

Table 4 – continued

ID	H β	σ H β	Mg $_1$	σ Mg $_1$	Mg $_2$	σ Mg $_2$	Mgb	σ Mgb	Fe5270	σ Fe5270
(1)	(2)	(3)	(4)	(5)	(6)	(7)	(8)	(9)	(10)	(11)
526	0.07177	0.00035	0.28018	0.00041	6.61085	0.01426	6.36810	0.01505
484	1.42297	0.03053	-0.02152	0.00060	0.06394	0.00070	2.11313	0.02707	1.99763	0.02954
6548	0.49610	0.74809	0.33930	0.01321	0.19814	0.01424	4.27093	0.53708	2.82585	0.53794
1181	2.67965	0.15076	-0.14580	0.00348	-0.16468	0.00409	1.62608	0.14106	0.95591	0.15715
1785	1.27569	0.01759	0.08821	0.00034	0.23752	0.00040	5.05040	0.01450	4.90434	0.01531
11860	3.35735	0.18422	0.00218	0.00383	0.71677	0.00498	1.14870	0.18832
5871	2.46747	0.21816	-0.14391	0.00494	-0.13159	0.00583	2.54280	0.19608	-3.16630	0.27030
6079	2.43809	0.12179	0.00421	0.00252	0.09106	0.00293	2.13766	0.11431	1.38027	0.12553
7299	2.76794	0.28393	0.02429	0.00565	0.01862	0.00644	1.54703	0.24870	1.59366	0.27111
7453	2.55815	0.25426	0.33351	0.00552	0.04884	0.00582	2.40941	0.22060	1.59301	0.24453
1214	0.87293	0.39518	0.35244	0.00791	0.12368	0.00840	4.41888	0.30498	2.33893	0.33750
951	2.63540	0.17575	0.37760	0.00394	0.03323	0.00411	1.96908	0.15781	1.04964	0.17669
2154	2.37938	0.15105	-0.01270	0.00307	0.04665	0.00356	1.68826	0.13859	1.57618	0.15162
1219	2.30168	0.16977	0.00382	0.00335	0.10030	0.00390	2.08078	0.15269
1716	5.05854	0.10029	-0.14959	0.00249	-0.18514	0.00293	0.75280	0.10358	0.69119	0.11499
8009	6.75657	0.03381	-0.03923	0.00087	1.03372	0.00000	3.29142	0.04321
654	1.30557	0.13419	0.09388	0.00254	0.87207	0.00328	3.71373	0.11508
1926	1.55802	0.13123	0.00368	0.00259	0.09613	0.00301	2.85480	0.11438	1.85090	0.12644
3	1.28607	0.11113	0.01817	0.00217	0.13638	0.00253	3.39220	0.09570	2.10816	0.10483
338	2.01372	0.02289	0.00469	0.00046	0.13770	0.00054	4.06774	0.01992	2.36165	0.02247
391	-0.05499	0.00098	-0.03216	0.00115	-0.11196	0.04611	-0.05713	0.05214
223	1.32851	0.07405	0.01308	0.00146	0.12933	0.00170	2.92818	0.06521	1.99434	0.07117
314	1.53876	0.04685	0.05839	0.00092	0.14398	0.00106	2.36277	0.04168	1.48794	0.04502
1325	1.38286	0.03284	0.01911	0.00065	0.11760	0.00076	2.96613	0.02891	2.10983	0.03182
294	3.66435	0.06909	-0.16222	0.00166	-0.16042	0.00196	1.62607	0.06790	1.63417	0.07465
4448	3.05098	0.12844	0.00424	0.00264	0.10155	0.00308	2.33764	0.11967	2.45124	0.12829
10218	1.31530	0.13068	0.00446	0.00254	0.11696	0.00296	3.15775	0.11213	1.56531	0.12445
3915	3.57394	0.10651	-0.00595	0.00227	0.07971	0.00264	2.14594	0.10230	2.04445	0.11183
813	2.27763	0.13500	-0.00951	0.00275	0.05576	0.00319	2.05247	0.12336	1.17302	0.13790
266	2.09607	0.05256	0.02996	0.00108	0.16865	0.00126	4.16956	0.04674	2.90924	0.05173
256	4.24373	0.03835	-0.01407	0.00086	0.03349	0.00100	1.08078	0.03967	0.92942	0.04408
1934	1.73745	0.16576	0.00724	0.00324	0.11142	0.00378	2.74445	0.14501	1.51214	0.15914
206	3.18473	0.09078	-0.01018	0.00191	0.04615	0.00222	1.23735	0.08817	1.39074	0.09595
407	1.15018	0.03032	0.03667	0.00059	0.15681	0.00069	3.28265	0.02631	2.81248	0.02832
1693	3.42373	0.22621	0.04329	0.00475	0.02734	0.00538	1.41763	0.20994	1.13405	0.22970
1818	2.65438	0.16302	0.17335	0.00351	0.03474	0.00385	1.87656	0.14822	0.65747	0.16729
6868	1.47979	0.07634	0.42762	0.00167	0.09404	0.00175	2.78518	0.06644	2.00677	0.07301
1210	2.84151	0.23267	0.34705	0.00510	0.05421	0.00537	2.18355	0.20595	1.06898	0.22814
2013	3.01131	0.22147	0.19284	0.00476	0.09281	0.00524	3.10394	0.19683	2.31253	0.21519
1161	2.34482	0.15288	0.08055	0.00315	0.02436	0.00355	1.03649	0.15329
6786	1.90330	0.13104	-0.00564	0.00264	0.08141	0.00308	2.39554	0.11849	1.28457	0.13231
12299	2.93148	0.17181	-0.03094	0.00354	0.03488	0.00412	1.47326	0.16069	0.86268	0.17882
888	1.75539	0.11167	0.01044	0.00223	0.10896	0.00260	3.10487	0.09823	1.68903	0.10945
7505	2.04387	0.27810	0.01887	0.00542	0.08254	0.00627	2.05155	0.24458
7573	3.99887	0.11547	-0.16686	0.00277	-0.18082	0.00327	0.98339	0.11491	1.17812	0.12547
452	0.07600	0.00035	0.33192	0.00041	6.23868	0.01469	4.41209	0.01611
10927	2.41246	0.03186	0.02152	0.00065	0.15032	0.00076	4.54685	0.02764	3.25964	0.03071
5964	2.46188	0.11564	0.00033	0.00239	0.06125	0.00278	1.85115	0.10823	1.20816	0.12015
1897	1.13113	0.04106	0.02704	0.00080	0.13332	0.00093	2.97601	0.03582	2.22412	0.03898
613	2.08808	0.14474	-0.00111	0.00290	0.06592	0.00336	2.13041	0.12993	1.31938	0.14343
641	1.19955	0.04389	0.03663	0.00085	0.13636	0.00099	2.54522	0.03865
651	1.21019	0.05873	0.46141	0.00128	0.12224	0.00133	2.87809	0.05105	2.13020	0.05557
720	1.44506	0.05036	0.02969	0.00099	0.14578	0.00115	2.56061	0.04530	2.35925	0.04723
4	1.93432	0.14130	-0.01842	0.00281	0.07474	0.00327	2.43530	0.12516	1.32923	0.13935
399	1.33173	0.02365	0.05027	0.00046	0.23893	0.00054	6.13691	0.01880	3.50330	0.02144
1282	1.50194	0.08294	-0.15261	0.00184	-0.13204	0.00218	2.61034	0.07305	-0.33876	0.09056
1081	1.05207	0.11905	0.01921	0.00233	0.12112	0.00272	3.02187	0.10336	1.80271	0.11394
829	1.06776	0.05433	0.01361	0.00106	0.10736	0.00123	2.52370	0.04758	2.10204	0.05178
4482	3.01291	0.12842	-0.00773	0.00272	0.05601	0.00316	1.71112	0.12339	0.79867	0.13770

Table 4 – continued

ID	H_{β}	σH_{β}	Mg_1	σMg_1	Mg_2	σMg_2	Mgb	σMgb	Fe5270	$\sigma Fe5270$
(1)	(2)	(3)	(4)	(5)	(6)	(7)	(8)	(9)	(10)	(11)
1486	1.39487	0.08907	0.00919	0.00177	0.11589	0.00206	2.98442	0.07839	1.80873	0.08705
3909	1.14953	0.13790	0.01219	0.00266	0.13415	0.00310	3.53451	0.11624	1.85187	0.12906
1087	1.36366	0.11818	0.01492	0.00234	0.12819	0.00272	3.21511	0.10309	2.01140	0.11367
387	2.43080	0.14175	-0.01197	0.00286	0.05819	0.00333	1.65046	0.13020	-5.06105	0.20487
778	1.49698	0.10983	0.01853	0.00216	0.12598	0.00252	3.12756	0.09562	1.89121	0.10542
2045	1.85734	0.12653	0.00135	0.00254	0.08299	0.00295	2.41215	0.11347	1.18041	0.12687
1292	1.33699	0.12083	0.01398	0.00238	0.10434	0.00277	2.91980	0.10516	1.82446	0.11643
242	1.79732	0.13878	-0.00059	0.00276	0.09248	0.00321	2.54538	0.12281	1.67391	0.13511
212	1.50184	0.04881	0.09768	0.00095	0.23621	0.00110	3.88277	0.04220	4.10027	0.04340
5412	1.30644	0.06089	0.01611	0.00120	0.11015	0.00139	2.63092	0.05350	2.10637	0.05834
574	2.79883	0.14897	0.36713	0.00337	0.02280	0.00352	1.55868	0.13625	1.08049	0.15132
78	2.86741	0.17928	0.29300	0.00396	0.03263	0.00420	1.87402	0.16125	1.15810	0.18010
1561	1.68997	0.13497	0.10795	0.00273	0.08656	0.00308	-1.51759	0.13994	1.69391	0.12911
1894	3.35560	0.18211	-0.01367	0.00380	0.53794	0.00482	4.45043	0.22861	1.09506	0.18772
881	3.78683	0.04534	-0.02727	0.00099	0.04604	0.00115	1.74615	0.04467	1.79704	0.04923
7014	2.37763	0.14366	-0.02200	0.00292	0.05087	0.00340	1.73564	0.13203	1.29846	0.14622
11907	2.84846	0.23225	-0.14932	0.00526	-0.14318	0.00620	2.03274	0.21047	1.19985	0.23761
523	1.77719	0.08943	-0.00010	0.00181	0.07916	0.00210	2.25041	0.08098	1.45859	0.08984
2229	3.78836	0.26392	0.00760	0.00535	0.07581	0.00622	2.00141	0.24222	1.80245	0.26055
2153	2.62474	0.15626	-0.05211	0.00331	-0.01073	0.00386	1.71805	0.14432	1.03627	0.15966
513	1.11320	0.03948	-0.02054	0.00080	0.12460	0.00093	3.80636	0.03375	2.48247	0.03747
5843	4.04459	0.03078	-0.00287	0.00067	0.11807	0.00078	3.34937	0.02922	1.77796	0.03266
11331	3.83852	0.16901	-0.00427	0.00358	0.02945	0.00415	1.08484	0.16388	0.65439	0.18158
1144	2.46969	0.09903	-0.02428	0.00204	0.04797	0.00238	1.91467	0.09191	1.01999	0.10294
1815	2.69190	0.13002	-0.00206	0.00270	0.05693	0.00314	1.80936	0.12187	0.82827	0.13635
616	2.14027	0.13974	-0.01746	0.00280	0.05768	0.00325	2.37608	0.12406	1.20654	0.14004
8076	2.26381	0.18873	-0.14617	0.00428	-0.14826	0.00505	1.96801	0.17150	0.92967	0.19099
1409	2.29504	0.21093	-0.07720	0.00448	-0.01780	0.00527	2.83997	0.18622	1.11685	0.20817

Table 5. Selected spectral indices and uncertainties.

ID	Fe5335	σ Fe5335	Fe5406	σ Fe5406	NaD	σ NaD	Al3953	σ Al3953
(1)	(2)	(3)	(4)	(5)	(6)	(7)	(8)	(9)
155	1.88008	0.05544	1.13882	0.04054	2.04970	0.03406
138	0.81074	0.02593	4.12518	0.02094	4.13757	0.08959
114	1.97289	0.04263	1.02490	0.03133
253	1.51201	0.03747	0.69764	0.02730
1468	0.84823	0.13686	0.69834	0.09912	1.86168	0.08544	2.70808	0.43285
367	0.60807	0.08541	0.20029	0.06286	1.48435	0.05619	3.41298	0.14671
327	1.95244	0.04120	1.13027	0.03021	3.26561	0.02444	3.25623	0.14144
346	1.06836	0.05323	0.87886	0.03839	1.95114	0.03249	3.73815	0.15558
356	4.72869	0.02187	5.82846	0.01238	2.10982	0.11406
221	1.93333	0.04331	1.14638	0.03170	2.04300	0.02633	3.68824	0.14965
207	0.36262	0.08785	1.54693	0.07733	3.20823	0.26721
291	4.29157	0.02001	1.40417	0.01533	6.36977	0.01129
306	1.05979	0.03108	4.15998	0.02479	-0.93592	0.29136
751	1.27704	0.16750	0.59313	0.12306	1.80957	0.10448	3.97421	0.57499
3791	1.66556	0.10151	0.88093	0.07444	1.97370	0.06277	2.11603	0.44516
1936	0.81900	0.15765	0.66817	0.11403	1.47505	0.09792	3.34221	0.51237
390	5.33949	0.01743	1.96846	0.01325	9.01046	0.00893	1.42806	0.10927
1511	7.84740	0.01242	4.83822	0.00930	8.81875	0.00699	0.42836	0.13982
1124	1.54715	0.03397	0.71771	0.02497
69	1.85099	0.04955	1.02622	0.03604	3.03424	0.17479
7677	0.96876	0.21559	0.82637	0.15647	1.10367	0.13828	0.76813	0.87924
51	0.93517	0.10502	0.17910	0.07758	1.82498	0.06769	3.64415	0.18788
488	0.47508	0.10135	0.48680	0.07362	1.59129	0.06554	3.05270	0.18440
7277	1.79542	0.12151	0.82457	0.09015	1.97723	0.08238	2.73261	0.47105
1351	5.78717	0.01269	1.88199	0.00983	8.36527	0.00651	0.02643	0.12503
573	0.89615	0.04462	2.33871	0.03734	3.21746	0.22140
505	1.56723	0.03514	0.76354	0.02595	1.98323	0.02190	3.43203	0.08805
1556	7.22957	0.01210	3.66878	0.00924	9.31503	0.00636	1.00106	0.12246
7498	7.49795	0.01150	2.03808	0.00946	7.66586	0.00651	0.14208	0.11679
917	1.87019	0.05849	0.96000	0.04283	2.00605	0.03592	3.76283	0.20126
1796	0.50466	0.27832	0.71101	0.19980	1.16686	0.17118	4.91702	1.00968
458	0.69960	0.02445	3.61287	0.01986	3.20395	0.08887
6761	1.64737	0.07901	1.04923	0.05763	2.14796	0.04823	3.03072	0.28683
566	4.20148	0.08733	2.79188	0.06456	4.22998	0.05104	0.28492	0.82609
439	3.70541	0.08057	2.10156	0.06051	3.70731	0.05016	0.76744	0.37679
619	0.84795	0.18939	0.32044	0.13842	1.66702	0.11823	5.39553	0.49262
1235	1.64902	0.10532	0.84878	0.07781	1.80787	0.06766	3.23324	0.29572
640	1.73364	0.03488	0.68479	0.02576	3.43285	0.02100	4.10011	0.08782
122	1.92711	0.07596	0.97030	0.05689	2.10646	0.04857	3.21900	0.20280
1035	1.29244	0.16604	0.70795	0.12118	1.81988	0.10179	4.49992	0.57375
787	2.18442	0.03773	1.14165	0.02770	3.78922	0.02172	3.56031	0.15401
292	1.58101	0.03606	0.75698	0.02647	5.34830	0.02072
258	1.78686	0.04892	3.11649	0.02908
2984	0.67412	0.12070	0.27678	0.08908	1.34410	0.07828	2.59936	0.25309
328	0.44214	0.09579	0.19050	0.07038	1.63522	0.06421
1060	2.22165	0.10880	1.16092	0.08134	2.07268	0.06969	3.35157	0.34487
1294	1.75503	0.11571	0.99874	0.08530	1.74806	0.07398	3.74682	0.32144
792	1.66604	0.09366	0.80134	0.06898	2.06663	0.05800	1.96757	0.40522
13	4.91128	0.02737	2.84901	0.02038	7.95423	0.01467	2.30609	0.16380
232	1.48008	0.10735	0.67056	0.07913	1.99062	0.06577	3.48433	0.40631
402	1.61127	0.03515	0.72657	0.02594
4126	1.51639	0.14848	0.79867	0.10869	1.97674	0.09164	4.21065	0.54356
1633	2.39855	0.08345	2.67346	0.05035	2.69732	0.36287
2001	1.42637	0.03466	0.73745	0.02559	2.94943	0.02116	4.62421	0.07610
1873	1.71704	0.07313	0.99498	0.05355	2.24143	0.04484	2.87170	0.26732
10387	1.17871	0.15119	0.58279	0.11081	1.57460	0.09422	6.02303	0.36726
1958	1.51552	0.13346	0.90350	0.09758	1.94411	0.08170	3.02844	0.60193
921	1.27145	0.10090	0.52541	0.07521	1.87059	0.06604	3.02401	0.19063

Table 5 – continued

ID	Fe5335	σ Fe5335	Fe5406	σ Fe5406	NaD	σ NaD	Al3953	σ Al3953
(1)	(2)	(3)	(4)	(5)	(6)	(7)	(8)	(9)
526	4.96871	0.01711	3.11902	0.01238	0.99159	0.13327
484	1.68761	0.03344	1.05350	0.02438	1.83346	0.02050	4.30435	0.09241
6548	2.70095	0.59014	2.37708	0.42203	2.56727	0.34309
1181	0.66861	0.12690	1.74240	0.11132	3.03023	0.46108
1785	3.13278	0.01758	1.78792	0.01291	2.57412	0.01040	2.11845	0.09314
11860	0.84356	0.21571	0.09819	0.15961	1.37398	0.13655	3.62595	0.71557
5871	12.32339	0.27252	-0.16567	0.18345	1.67359	0.15338	2.56151	0.98518
6079	1.01860	0.14303	0.74467	0.10416	1.81616	0.08961	4.73762	0.35331
7299	0.55601	0.31312	0.67329	0.22237	1.48273	0.18879	6.10641	0.96179
7453	0.59866	0.28284	-0.09022	0.20780	1.90269	0.17100	3.71238	1.13530
1214	1.44650	0.38574	1.28500	0.27374	2.13300	0.22363	2.91973	1.82234
951	1.12423	0.19938	0.34240	0.14689	1.45882	0.12586	4.41565	0.57983
2154	1.05292	0.17371	0.29589	0.12803	1.61639	0.10815	4.87071	0.43522
1219	1.60980	0.18361	0.84906	0.13545	2.39961	0.11474	4.76836	0.58302
1716	0.17035	0.09490	1.56270	0.08467	3.15587	0.24504
8009	5.24613	0.04609	2.94921	0.03593	4.02323	0.09952
654	3.27638	0.12831	2.33312	0.09376	2.96788	0.07752	5.02895	0.79250
1926	1.40006	0.14373	2.29584	0.08678	2.97128	0.57746
3	1.63310	0.11896	0.90890	0.08769	2.06072	0.07176	4.51402	0.44895
338	2.61543	0.02510	1.10601	0.01865	2.71342	0.01536	3.59507	0.07471
391	-0.03744	0.06012	0.00765	0.04419	1.39905	0.04257
223	1.73680	0.08037	0.97835	0.05897	1.86579	0.04919	3.68973	0.28871
314	2.70134	0.04824	1.51584	0.03574	3.18568	0.02930	3.37818	0.18496
1325	1.68266	0.03606	0.81257	0.02656	3.29840	0.02138	3.12163	0.11315
294	0.59059	0.06225	1.54293	0.05534	3.12744	0.19310
4448	2.48048	0.14355	0.98286	0.10841	2.88919	0.08917	4.32998	0.52777
10218	1.61451	0.13955	0.79297	0.10246	2.01120	0.08477	4.54057	0.37617
3915	1.91833	0.12593	0.89782	0.09418	1.99952	0.08046	2.67857	0.43378
813	0.87306	0.15690	0.66021	0.11404	1.93974	0.09731	3.47166	0.49736
266	2.58337	0.05849	1.84446	0.04318	2.84290	0.03667	3.43362	0.17819
256	1.13201	0.05006	0.45228	0.03707	1.29847	0.03322	3.67455	0.08159
1934	1.46685	0.17853	0.94456	0.13000	2.08951	0.10892	-0.28106	1.27920
206	1.05595	0.10937	0.41655	0.08117	1.60935	0.06918	3.64951	0.26288
407	2.07219	0.03200	1.27635	0.02339	3.89991	0.01854	2.33879	0.13003
1693	0.53781	0.26314	0.72509	0.18727	1.53842	0.16221	4.80290	0.74823
1818	0.99156	0.18734	0.76916	0.13587	1.63487	0.11787	3.46074	0.53511
6868	1.54993	0.08306	0.88462	0.06074	2.01688	0.05101	3.70292	0.28231
1210	0.97807	0.25830	0.84180	0.18672	1.66924	0.16140	2.18723	1.03946
2013	1.79819	0.24500	1.24277	0.18039	2.33288	0.15047	4.91327	1.01110
1161	1.06192	0.17362	0.53570	0.12673	1.89938	0.10848	4.05533	0.47317
6786	0.70701	0.15157	0.43311	0.10978	1.91228	0.09420
12299	0.21969	0.20478	-0.00496	0.15019	1.69899	0.12646	4.67488	0.50955
888	1.52332	0.12348	0.86581	0.09018	2.10037	0.07573	4.78713	0.45893
7505	0.90818	0.30002	0.46721	0.22145	1.68895	0.18433	6.79087	0.80568
7573	-1.36363	0.21260	0.55254	0.10294	1.73143	0.09011	3.80224	0.32946
452	3.46056	0.01791	2.73758	0.01296	5.01835	0.01012	3.54754	0.07812
10927	4.45045	0.03333	1.48507	0.02565	10.72231	0.01686	3.88414	0.10960
5964	0.87000	0.13706	0.43844	0.10055	1.49708	0.08654	4.76196	0.31327
1897	1.87926	0.04391	1.08969	0.03228	3.16729	0.02618	3.49782	0.14693
613	1.11736	0.16330	0.80905	0.11813	1.62871	0.10046	3.55419	0.53072
641	1.84637	0.04632	0.78638	0.03428	4.24248	0.02708	2.90108	0.17047
651	1.67528	0.06286	1.04275	0.04599	2.21284	0.03838
720	2.45714	0.05268	1.25471	0.03902	2.85732	0.03213	3.27849	0.20619
4	1.42512	0.15674	0.16262	0.11870	2.06199	0.09575	4.77959	0.51265
399	3.38575	0.02374	1.65304	0.01762	7.78670	0.01240	2.55373	0.13061
1282	0.85223	0.06550	2.08299	0.05516	3.16112	0.35116
1081	1.65744	0.12883	1.03263	0.09397	1.97172	0.07904	3.44093	0.59470
829	1.74458	0.05865	0.96855	0.04300	2.04398	0.03582	3.09130	0.21529
4482	0.82764	0.15675	1.79999	0.09794	4.19127	0.40209

Table 5 – continued

ID	Fe5335	σ Fe5335	Fe5406	σ Fe5406	NaD	σ NaD	Al3953	σ Al3953
(1)	(2)	(3)	(4)	(5)	(6)	(7)	(8)	(9)
1486	1.79260	0.09804	1.10070	0.07184	1.62756	0.06126	2.37508	0.39374
3909	1.55553	0.14598	1.78727	0.08849	3.77577	0.74441
1087	1.56550	0.12960	0.98579	0.09431	2.00786	0.07938	3.51205	0.49106
387	0.82944	0.16243	0.79228	0.11748	1.62529	0.10130	3.79242	0.48981
778	1.74358	0.11887	1.00316	0.08732	1.74430	0.07325	2.93407	0.53113
2045	1.09128	0.14326	0.61309	0.10526	1.86543	0.08843	3.23094	0.50473
1292	1.47703	0.13244	0.73218	0.09733	2.14589	0.08061	2.48720	0.59800
242	1.22167	0.15383	0.38858	0.11451	1.87789	0.09458	6.53663	0.28232
212	3.73995	0.04812	5.92878	0.02682	2.71097	0.34024
5412	1.68524	0.06605	0.96588	0.04844	2.36532	0.04005	3.03503	0.25712
574	0.77934	0.17349	0.37815	0.12625	1.48217	0.10809	3.75212	0.48791
78	0.63643	0.20610	0.63973	0.14822	1.80273	0.12771	3.05079	0.64166
1561	1.47053	0.14637	0.51445	0.10777	1.77911	0.09100	0.18369	0.79269
1894	0.39047	0.21706	0.55319	0.15640	1.60446	0.13524	3.93562	0.64747
881	0.92866	0.05714	0.77508	0.04178	1.70466	0.03691	3.64786	0.11143
7014	1.05350	0.16653	0.62449	0.12075	1.72585	0.10407	4.24166	0.46861
11907	0.21974	0.19226	1.72373	0.16724	3.96968	0.89711
523	1.27628	0.10225	0.63888	0.07516	1.66726	0.06379	2.70793	0.32215
2229	1.48455	0.30012	0.09952	0.22388	1.84882	0.18548	4.19124	1.13152
2153	1.54874	0.11257	4.85807	0.44442
513	2.05710	0.04221	1.49305	0.03065	-0.77358	0.02760
5843	2.25559	0.03652	1.42794	0.02663	2.75761	0.02204	3.79642	0.09944
11331	0.25566	0.20857	0.17199	0.15184	1.42899	0.13115	3.50476	0.53636
1144	1.00494	0.11726	1.65590	0.07363	4.00095	0.27559
1815	0.81040	0.15481	0.42560	0.11344	1.55366	0.09775	3.42074	0.42193
616	1.06674	0.15872	0.51563	0.11617	1.98283	0.09716	3.63461	0.49448
8076	0.19108	0.15584	1.45762	0.13649	4.66239	0.69923
1409	0.79311	0.16702	1.63869	0.14313	1.58806	1.00579